Nanoscale Thermoelectrics

Branislav K. Nikolić
Department of Physics and Astronomy, University of Delaware,
Newark, DE 19716, U.S.A.

http://wiki.physics.udel.edu/phys824

Thermoelectric Energy Conversion: Fundamentals and Applications

Fundamentals

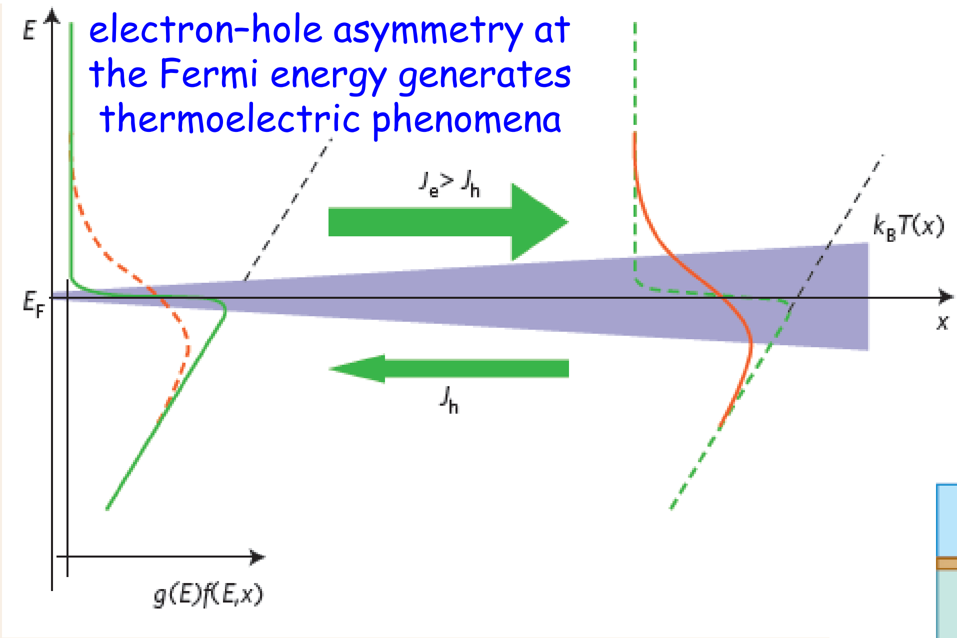

$$K = K_{\rm el} + K_{\rm ph}$$

$$\kappa = \kappa_{\rm el} + \kappa_{\rm ph}$$

bulk

$$\begin{pmatrix} \mathbf{E} \\ \mathbf{Q} \end{pmatrix} = \begin{pmatrix} 1/\sigma & S \\ \Pi & K \end{pmatrix} \begin{pmatrix} J \\ -\nabla T \end{pmatrix}$$

constrictions and interfaces

$$\begin{pmatrix} -\Delta V \\ \mathbf{Q} \end{pmatrix} = \begin{pmatrix} 1/G & S \\ \Pi & \kappa \end{pmatrix} \begin{pmatrix} I \\ -\Delta T \end{pmatrix}$$

Applications

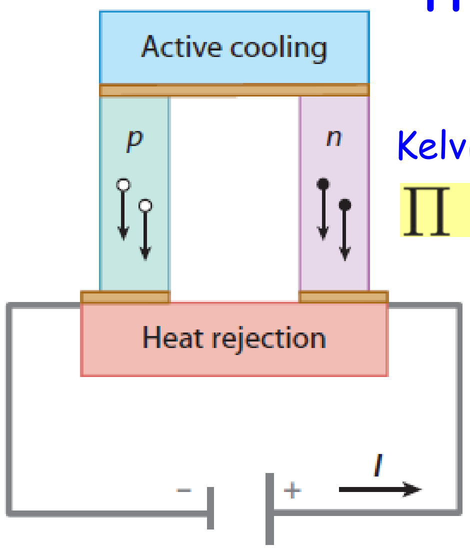

Refrigeration mode

Kelvin-Onsager

$$\Pi = ST$$

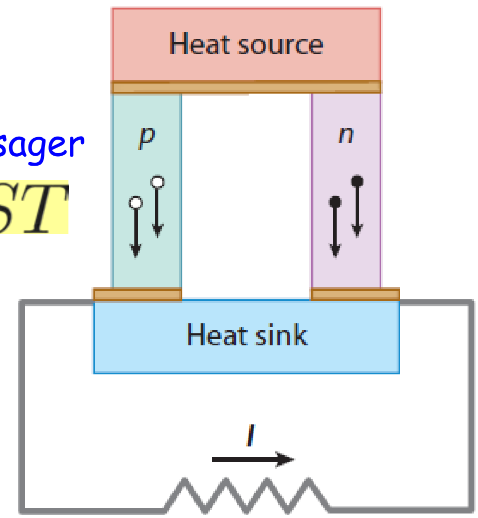

Power generation mode

Thermoelectric Figure of Merit ZT in the Linear-Response Regime

$$ZT = \frac{S^2 G T}{\kappa_{\rm el} + \kappa_{\rm ph}}$$

$$ZT = \frac{(S_p - S_n)^2 T}{[(\kappa_n/\sigma_n)^{1/2} + (\kappa_p/\sigma_p)^{1/2}]^2}$$

- In the linear-response regime (i.e., close to equilibrium) one operates close to the small voltage $V = -S\,\Delta T$ which exactly cancels the current induced by the small temperature bias ΔT
- As $ZT \rightarrow \infty$, the efficiency approaches the ideal Carnot value

$\eta_C = 1 - T/(T + \Delta T)$

- thus, in the linear-response regime $\Delta T \ll T$ typically investigated for bulk materials, the efficiency stays low $\eta_C = \Delta T / T$ even if ZT can be made very large

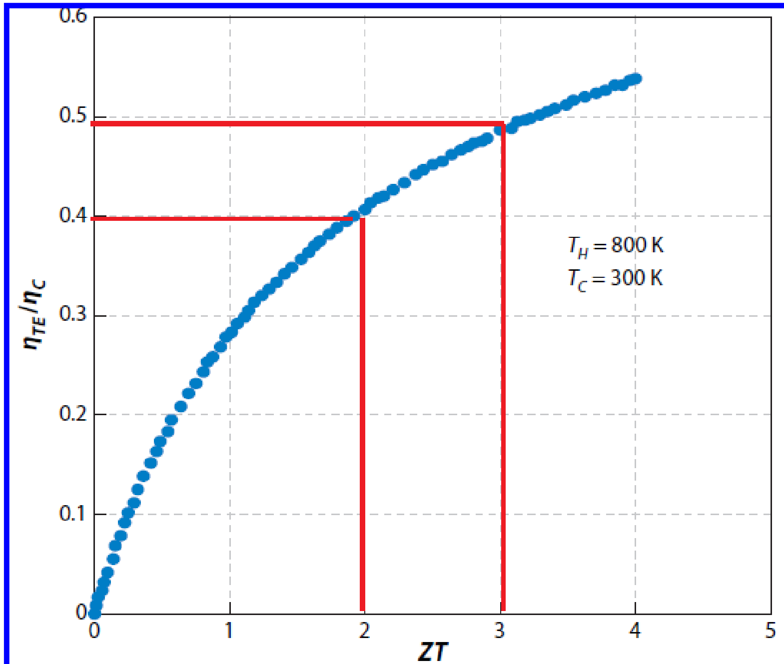

$$\eta_{\rm TE} = \frac{W}{Q_H} = \frac{T_H - T_C}{T_H}\left(\frac{(1+ZT_M)^{1/2} - 1}{(1+ZT_M)^{1/2} + T_C/T_H}\right)$$

Ultimate pragmatic goal:
devices with $ZT \approx 2$–3 that are stable over a broad temperature range with low parasitic losses

Decades of Little Progress in Increasing ZT of Bulk Materials

An inconvenient truth about thermoelectrics

Nature Mater. **8**, 83 (2009)

Cronin B. Vining

Despite recent advances, thermoelectric energy conversion will never be as efficient as steam engines. That means thermoelectrics will remain limited to applications served poorly or not at all by existing technology. Bad news for thermoelectricians, but the climate crisis requires that we face bad news head on.

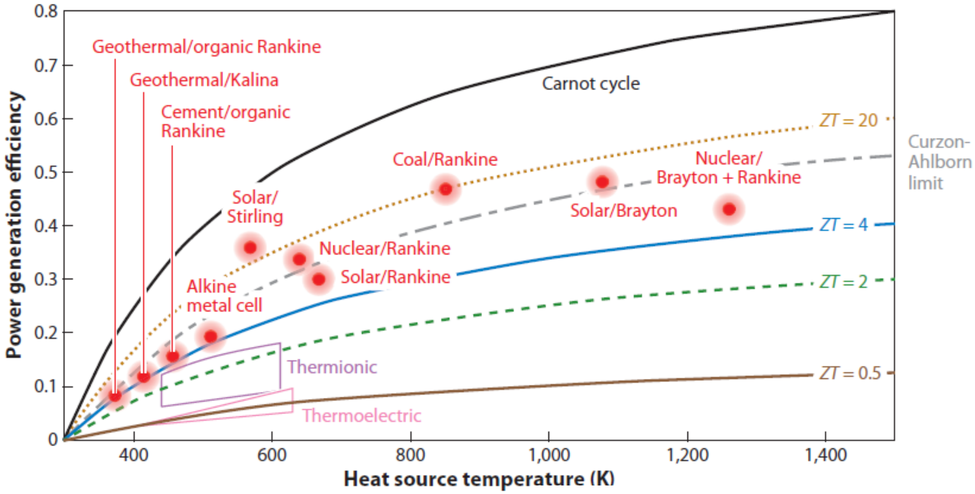

"phonon glass-electron crystal"

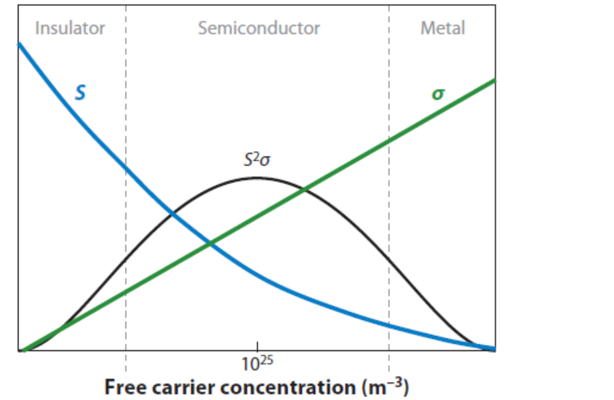

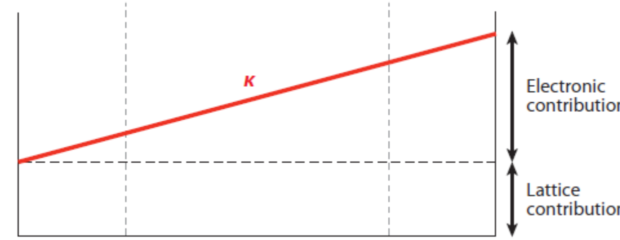

complex bulk materials

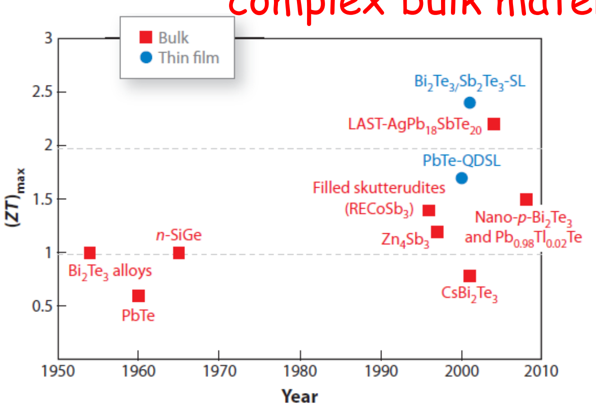

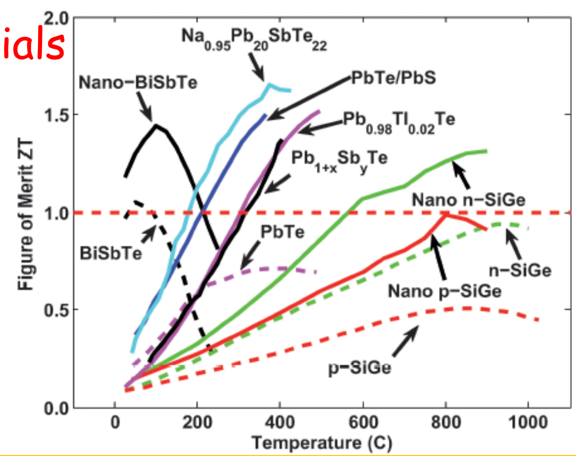

Mahan-Sofo mechanism

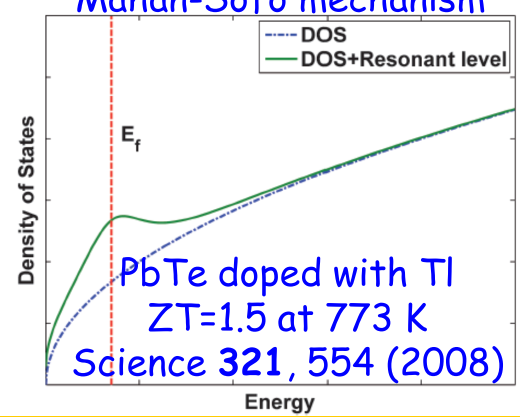

PbTe doped with Tl
ZT=1.5 at 773 K
Science **321**, 554 (2008)

Graphene as a Building Block of Nanoscale and Low-Dimensional Devices

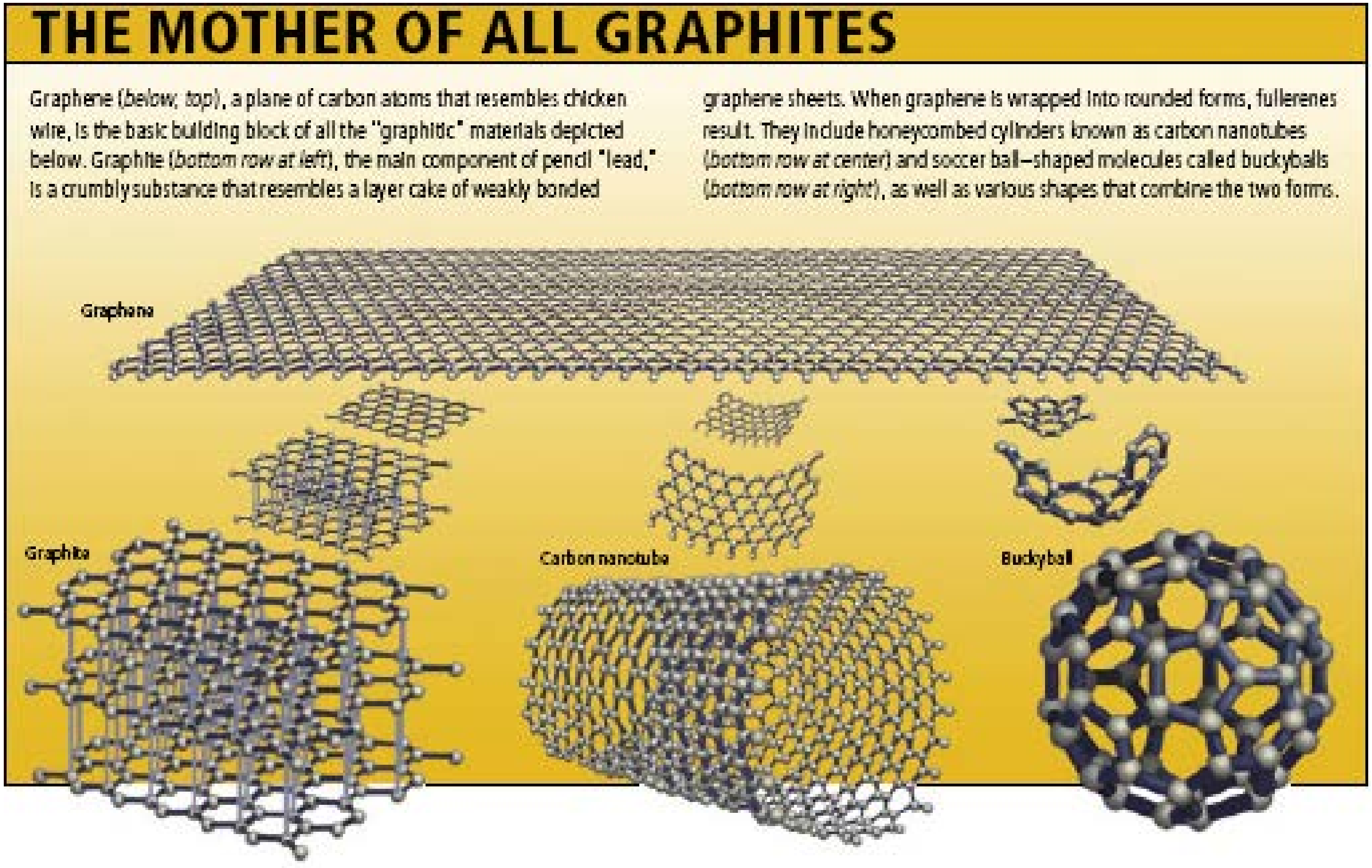

Large-Area Graphene is not Suitable for Thermoelectric Applications

Balandin Lab, New J. Phys. **11**, 095012 (2009)

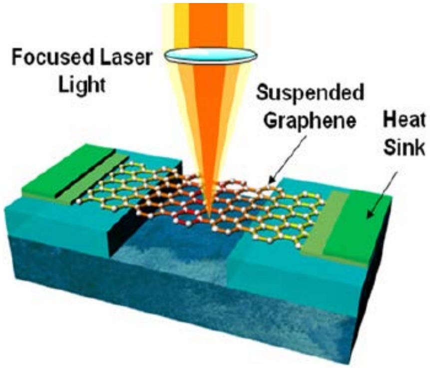

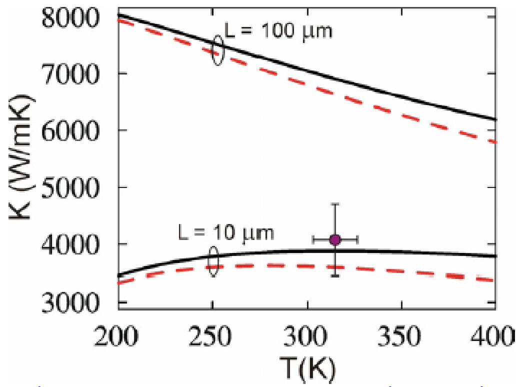

Kim Lab, PRL **102**, 096807 (2009)

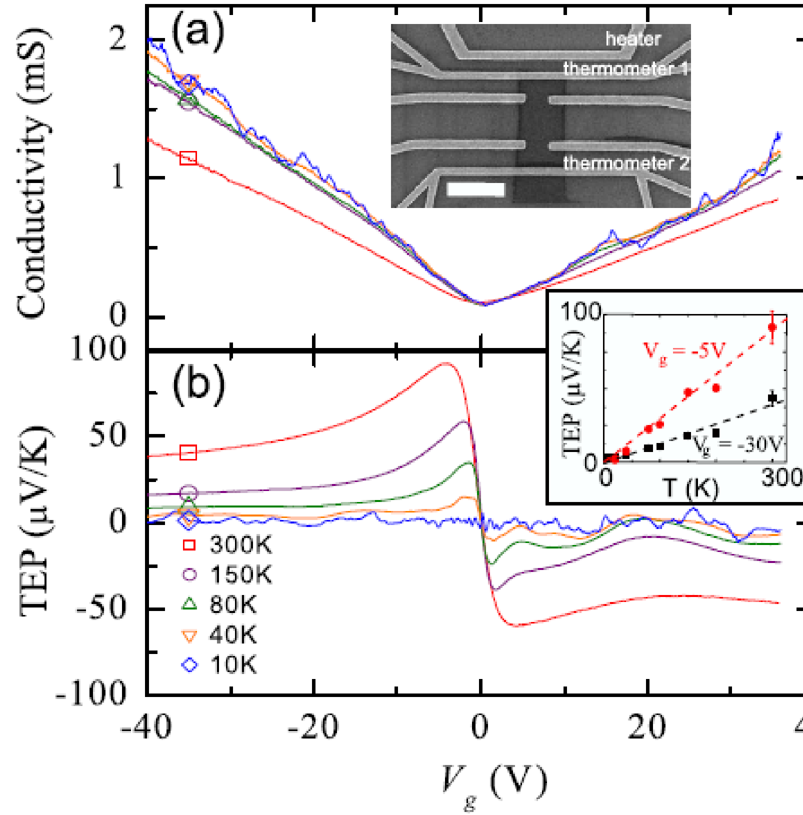

Shi Lab, ACS Nano **5**, 321 (2011); Science **328**, 213 (2010)

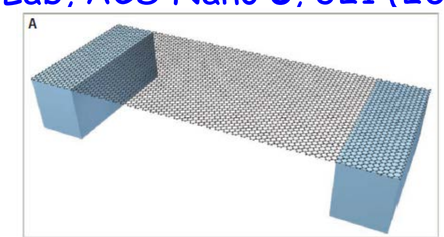

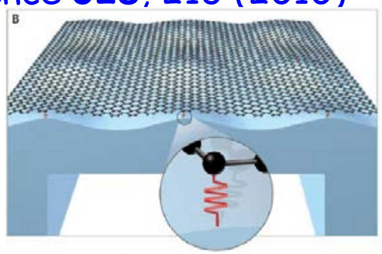

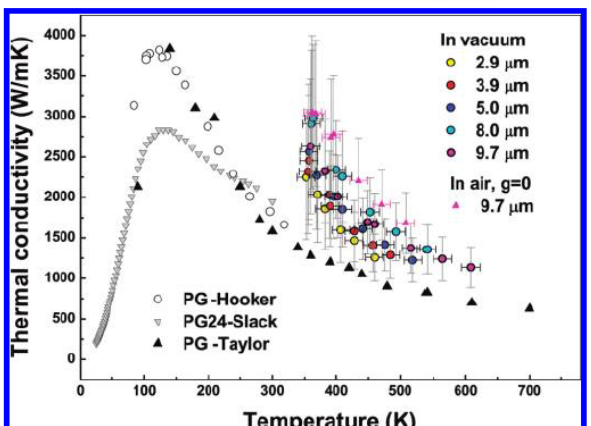

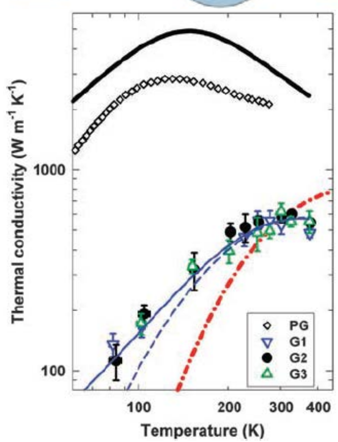

nature materials | REVIEW ARTICLE

PUBLISHED ONLINE: 22 JULY 2011 | DOI: 10.1038/NMAT3064

Thermal properties of graphene and nanostructured carbon materials

Alexander A. Balandin

Zigzag and Chiral GNRs with Nanopore Arrays as Potentially High-ZT Thermoelectrics

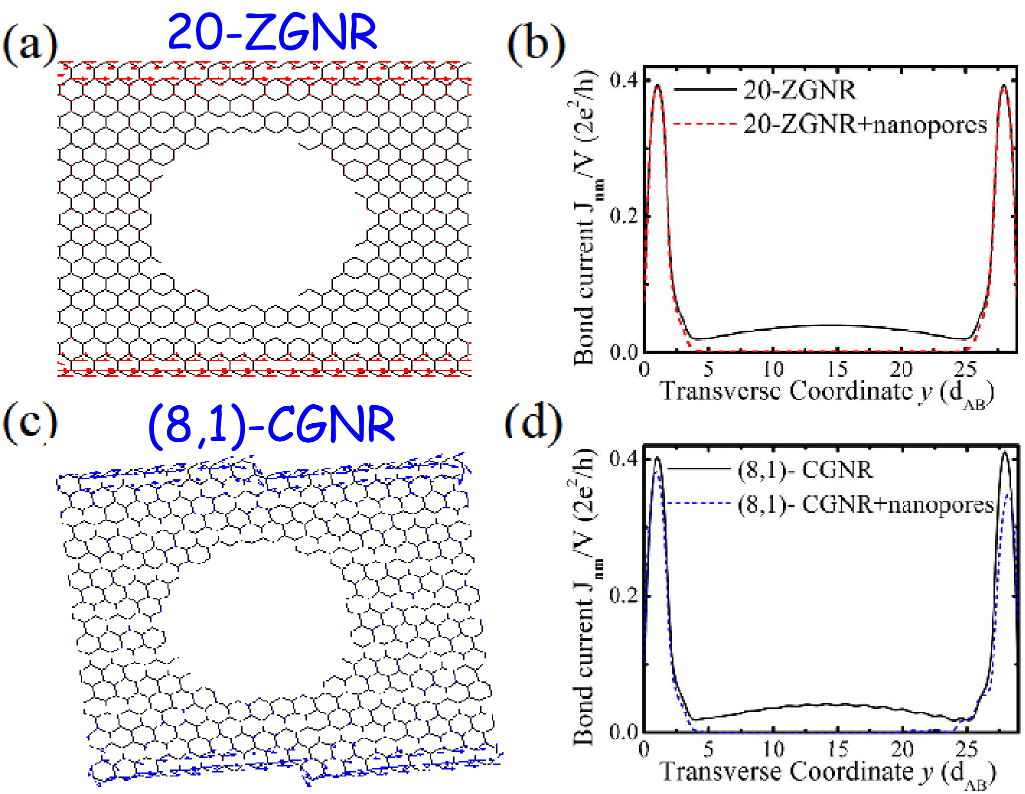

$L \simeq 1.2\ \mu m$

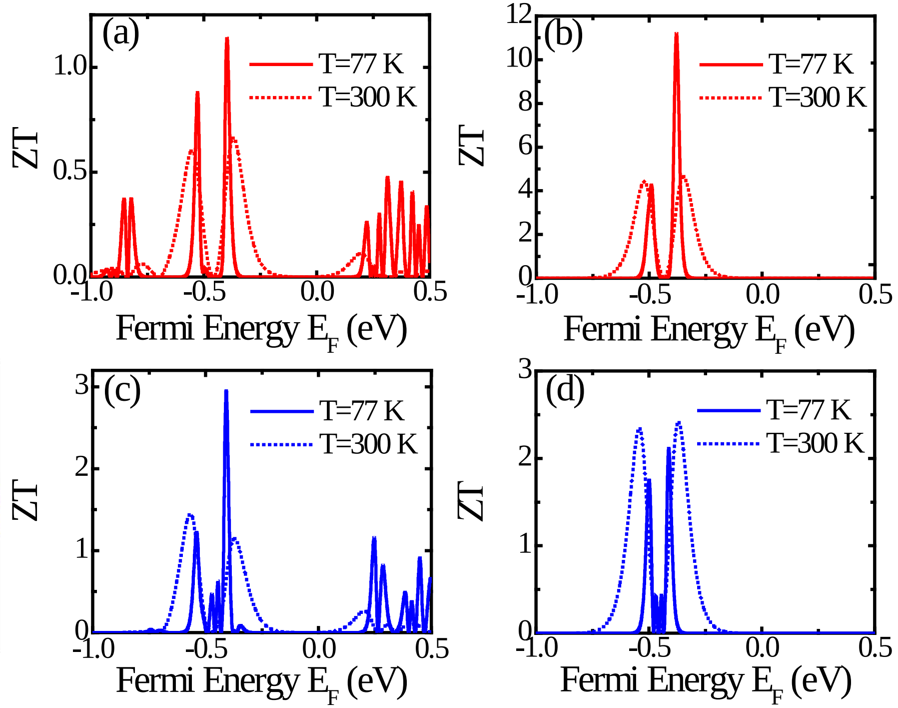

PRB ???, (2012)

NEGF Fundamentals

❑Basic NEGF quantities:

density of available quantum states:

$$G^r_{\sigma\sigma'}(t,t') = -\frac{i}{\hbar}\Theta(t-t')\langle\{\hat{c}_{\mathbf{r}\sigma}(t), \hat{c}^\dagger_{\mathbf{r}'\sigma'}(t')\}\rangle$$

how are those states occupied:

$$G^<_{\sigma\sigma'}(t,t') = \frac{i}{\hbar}\langle\hat{c}^\dagger_{\mathbf{r}'\sigma'}(t')\hat{c}_{\mathbf{r}\sigma}(t)\rangle$$

❑NEGFs for steady-state transport:

$$G^r(t,t') \to G^r(t-t') \xrightarrow{\text{FT}} G^r(E)$$

$$G^<(t,t') \to G^<(t-t') \xrightarrow{\text{FT}} G^<(E)$$

$$\boldsymbol{D}_{\text{eq}} = -\frac{1}{\pi}\int_{-\infty}^{+\infty} dE\, \text{Im}\,\mathbf{G}^r(E) f(E-E_F)$$

$$\boldsymbol{D}_{\text{neq}} = \frac{1}{2\pi i}\int_{-\infty}^{+\infty} dE\, \mathbf{G}^<(E)$$

❑NEGF (quantum) vs. Boltzmann (semiclassical) nonequilibrium statistical mechanics:

$$\begin{aligned} G^r(E) &= [E - H - \Sigma^r_{\text{leads}} - \Sigma^r_{\text{int}}]^{-1} \\ G^<(E) &= G^r(E)[\Sigma^<_{\text{leads}}(E) + \Sigma^<_{\text{int}}(E)]G^a(E) \end{aligned}$$

$$\mathbf{v}\cdot\nabla f + \mathbf{F}\cdot\nabla_{\mathbf{k}} f = I_{\text{coll}}[f]$$

$$\mathbf{j} = 2_s e \int \frac{d^3\mathbf{k}}{(2\pi)^3}\mathbf{v}(\mathbf{k}) f(\mathbf{k})$$

❑NEGF-based current expression for two-terminal nanostructures:

$$I_\alpha = \frac{2e}{h}\int dE\, \text{Tr}\,\{\Sigma^<_\alpha(E)G^>(E) - \Sigma^>_\alpha(E)G^<(E)\}$$

Meir-Wingreen formula

$$I(V_{ds}) = \frac{2e}{h}\int_{-\infty}^{+\infty} dE\, \text{Tr}\,\{\boldsymbol{\Gamma}_R(E,V_{ds})\mathbf{G}^r_{S1}\boldsymbol{\Gamma}_L(E,V_{ds})\mathbf{G}^a_{1S}\}\,[f(E-\mu_L)-f(E-\mu_R)]$$

Landauer-Büttiker-type formula (phase-coherent transport where Coulomb interaction is treated at the mean-field level)

Electronic Thermopower, Conductance and Thermal Conductance via NEGF

❑Electronic transmission and its integrals:

$$\begin{aligned} \mathcal{T}_{\mathrm{el}}(E) &= \mathrm{Tr}\left\{\mathbf{\Gamma}_R(E)\mathbf{G}(E)\mathbf{\Gamma}_L(E)\mathbf{G}^\dagger(E)\right\} \\ \mathbf{G}(E) &= [E\mathbf{S} - \mathbf{H} - \mathbf{\Sigma}_L(E) - \mathbf{\Sigma}_R(E)]^{-1} \\ H_{ij} &= \langle\phi_i|\hat{H}_{\mathrm{KS}}|\phi_j\rangle,\ S_{ij} = \langle\phi_i|\phi_j\rangle \\ \mathbf{\Gamma}_{L,R}(E) &= i[\mathbf{\Sigma}_{L,R}(E) - \mathbf{\Sigma}^\dagger_{L,R}(E] \end{aligned}$$

$$K_n(\mu) = \frac{2}{h}\int_{-\infty}^{\infty} dE\, \mathcal{T}_{\mathrm{el}}(E)(E-\mu)^n\left(-\frac{\partial f(E,\mu)}{\partial E}\right)$$

❑Electronic conductance, thermopower, and thermal conductance:

$$G = e^2 K_0(\mu)$$

$$S = K_1(\mu)/[eTK_0(\mu)]$$

$$\frac{-\partial f(E,\mu)}{\partial E} = \{2k_BT[1+\cosh(E-\mu)/k_BT]\}^{-1}$$

$$\kappa_{\mathrm{el}} = \{K_2(\mu) - [K_1(\mu)]^2/K_0(\mu)\}/T$$

JCEL **11**, 78 (2012)

Third-Nearest-Neighbor π-Orbital Tight-Binding Hamiltonian For Graphene

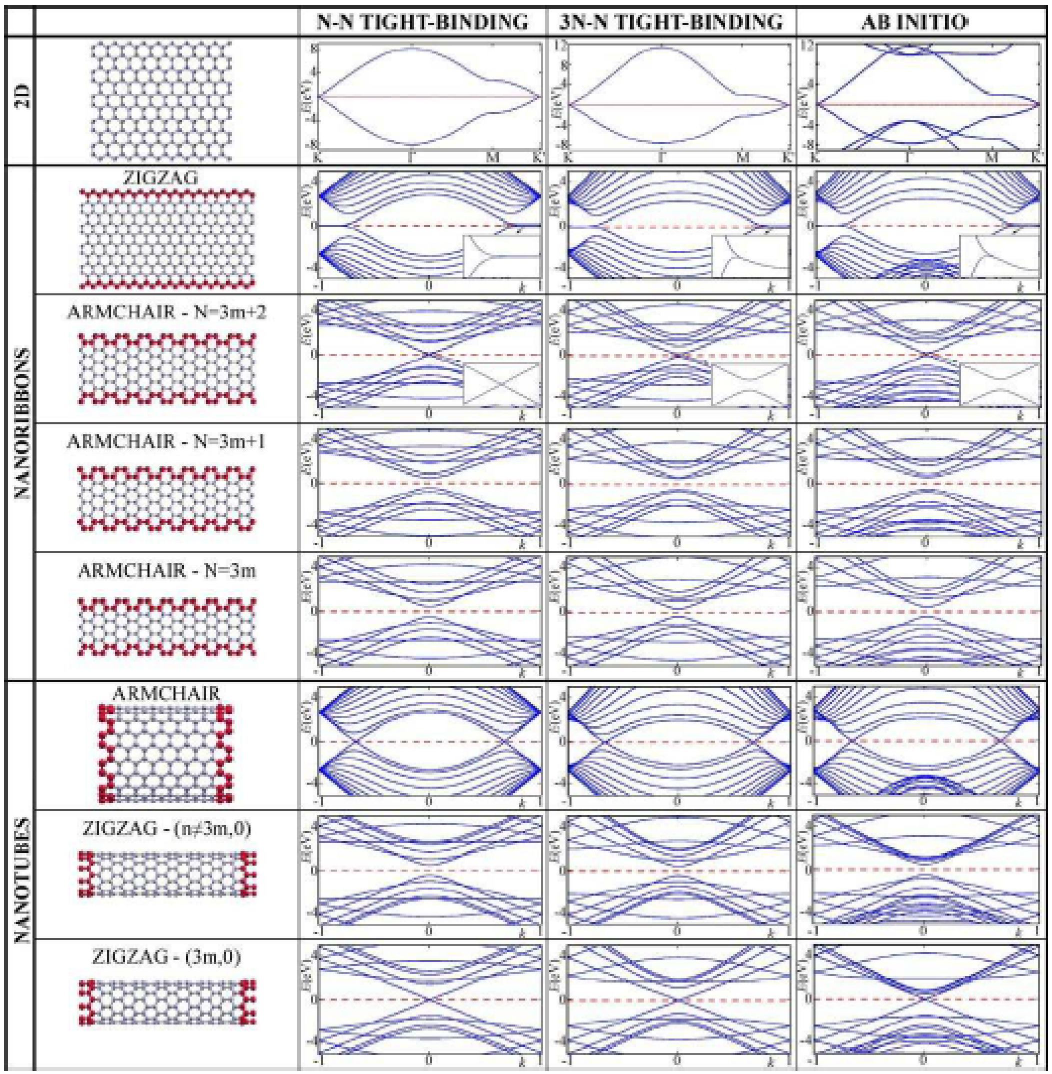

Nano Research 1, 361 (2008)

$$\hat{H} = \sum_{\mathbf{n}} \varepsilon_{\mathbf{n}} \hat{c}^{\dagger}_{\mathbf{n}} \hat{c}_{\mathbf{n}} - \sum_{\mathbf{n},\mathbf{m}} t^{\mathbf{m}}_{\mathbf{n}} \hat{c}^{\dagger}_{\mathbf{n}} \hat{c}_{\mathbf{m}}$$

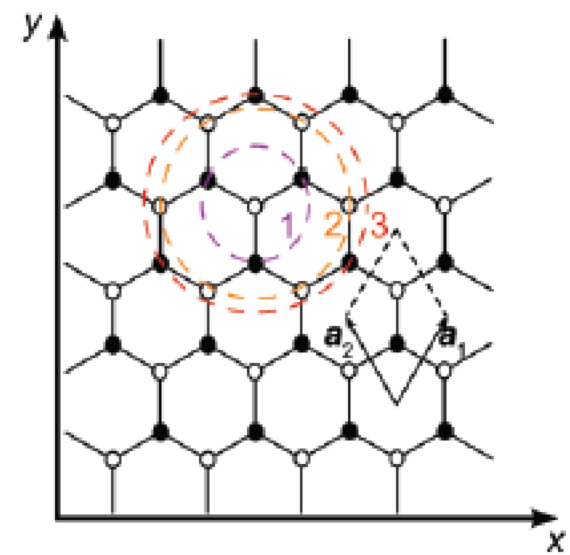

$$t_{\mathbf{n}}^{\mathbf{n}+\mathbf{d}_{AB}} = 2.7 \text{ eV}$$

$$t_{\mathbf{n}}^{\mathbf{n}+\mathbf{d}_{AA}} = t_{\mathbf{n}}^{\mathbf{n}+\mathbf{d}_{BB}} = 0.2 \text{ eV}$$

$$t_{\mathbf{n}}^{\mathbf{n}+\mathbf{d}_{AB'}} = 0.18 \text{ eV}$$

Zigzag GNR: Fundamentals

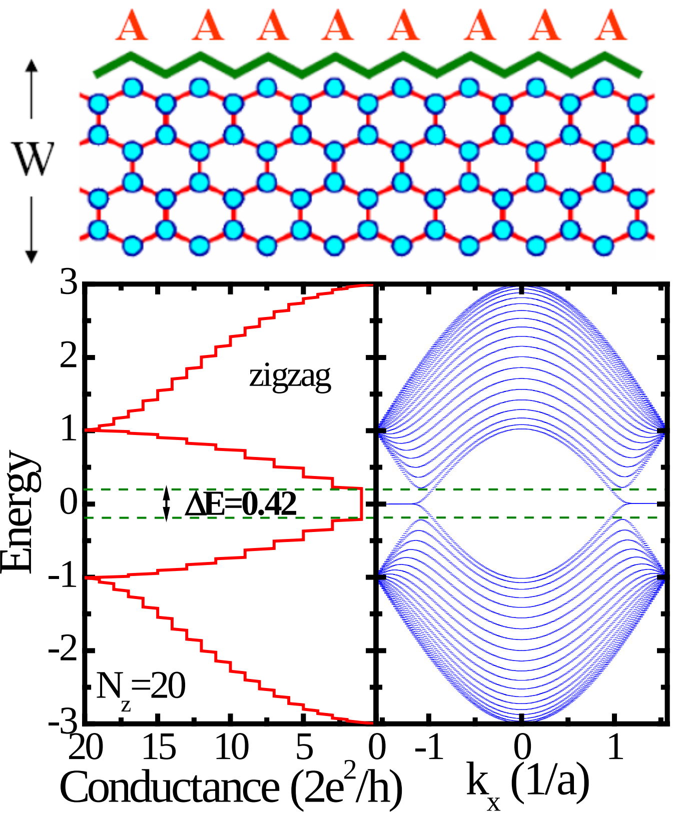

Areshkin & White, Nano Lett. **7**, 3253 (2007)

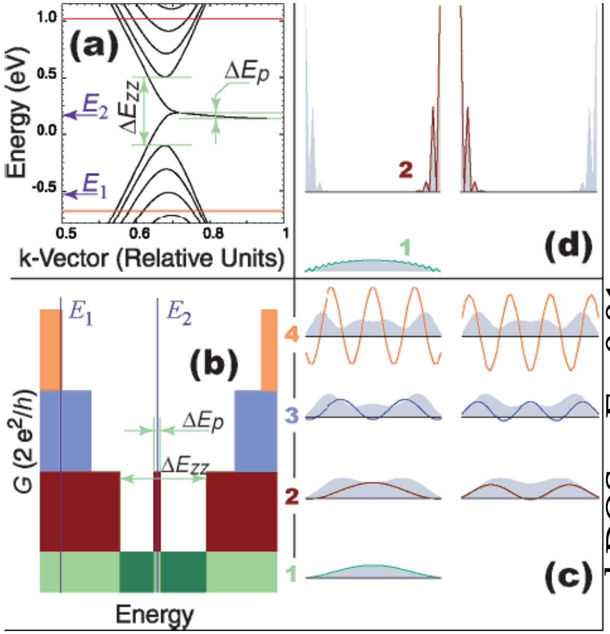

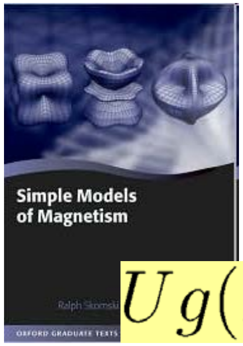

$Ug(E_F) > 1$

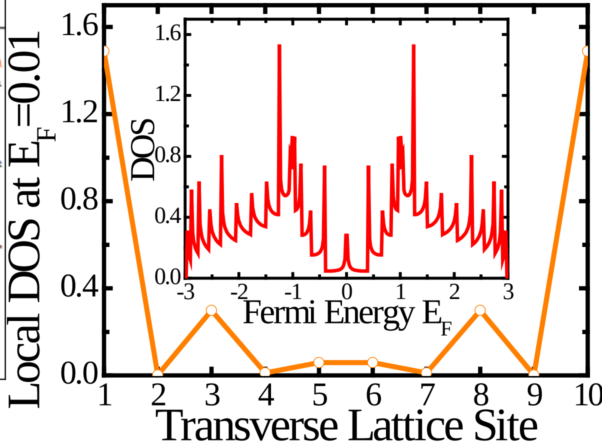

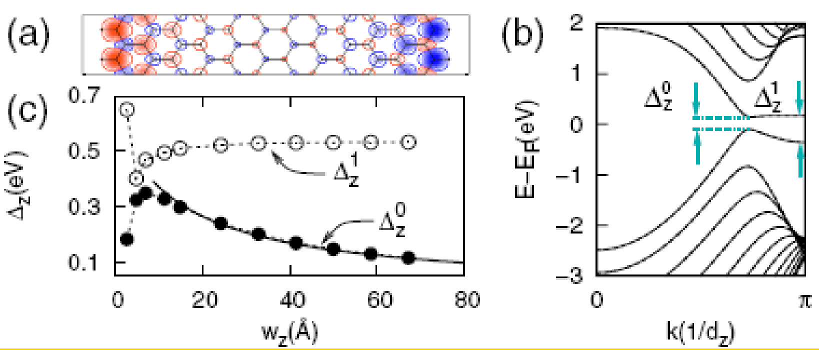

Son, Cohen, and Louie, PRL **97**, 216803 (2006)

First-Principles Quantum Transport Modeling Charge, Heat and Spin Transport: NEGF+DFT

DFT

Kohn-Sham Hamiltonian

$$\left[\frac{-1}{2}\nabla^2+V_H+V_{XC}\right]\Phi_i=\epsilon_i\Phi_i$$

$$H[n]=\frac{-1}{2}\nabla^2+V_H+V_{XC}$$

Leads' self-energies

$$\Sigma_L=H_{ML}g_L H_{LM}$$

$$\Sigma_R=H_{MR}g_R H_{RM}$$

$$\Gamma_{L,R}=i[\Sigma_{L,R}-\Sigma^{\dagger}_{L,R}]$$

$g_{L,R}\equiv$ Leads' surface Green function

Scatterer's Green Function

$$G=[ES-H[n]-\Sigma_L-\Sigma_R]^{-1}$$

NEGF

Non-equilibrium density matrix

$$D=\frac{-1}{\pi}\int dE\,\mathrm{Im}[G]\,f_F(E-\mu_L)+\frac{1}{2\pi}\int dE\,[G\Gamma_R G^{\dagger}][f_F(E-\mu_R)-f_F(E-\mu_L)]$$

Current

$$I=\frac{e}{h}\int d\varepsilon\,[\Gamma_L G^{\dagger}\Gamma_R G](n_F(\varepsilon-\mu_L)-n_F(\varepsilon-\mu_R))$$

open source:
GPAW!
Smeagol – Non-equilibrium Electronic Transport
Trans siesta
ALACANT – ALicante Ab initio Computation Applied to NanoTransport

commercial:
QuantumWise
NANODCAL

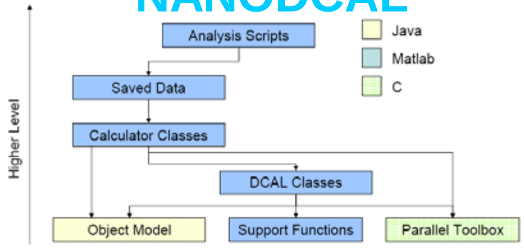

How to Apply NEGF-DFT to Devices Containing Thousands of Atoms

Main Obstacles: Computational complexity O(N[3]) of matrix inversion to get the retarded GF and hard-to-converge real-axis integration of spiky NEGF expressions to get the density matrix

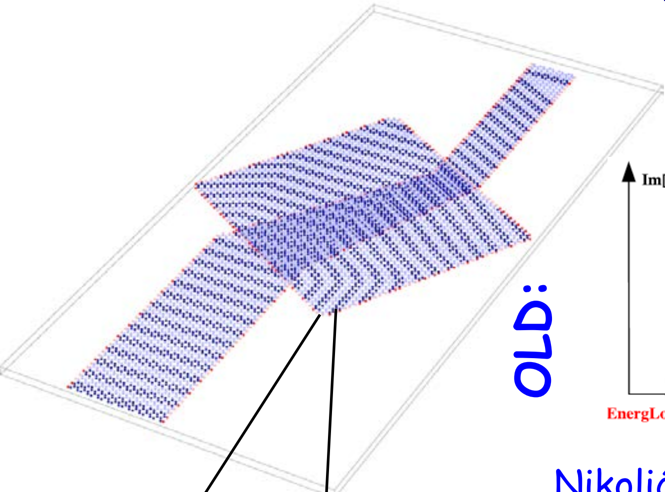

$\mathbf{H}_{i,i}$ $\mathbf{H}_{i+1,i+1}$

$\mathbf{H}_{i,i+1}$

Construct the layer retarded Green functions needed for charge density using recursive algorithms with O(N) complexity

OLD:

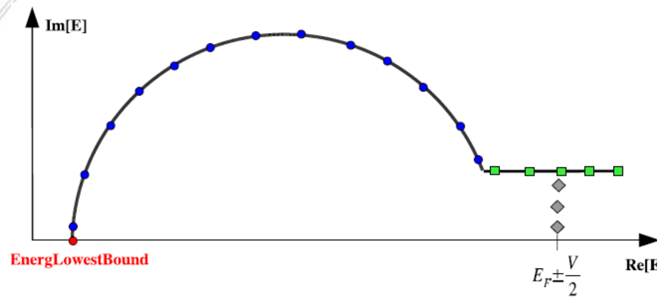

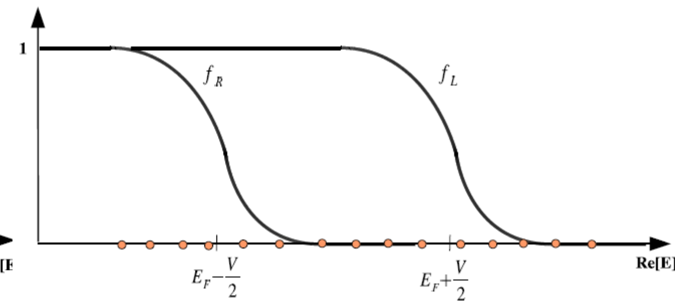

Nikolić group, PRB **81**, 155450 (2010)

$$\boldsymbol{\rho}_{\rm eq} = -\frac{1}{\pi}{\rm Im}\left[\sum_{j=1}^{N_{\rm pole}} 2\pi i \, {\rm Res}\left[\tilde{f}(z)\right]_{z=Z_j} \mathbf{G}^r(Z_j)\right],$$

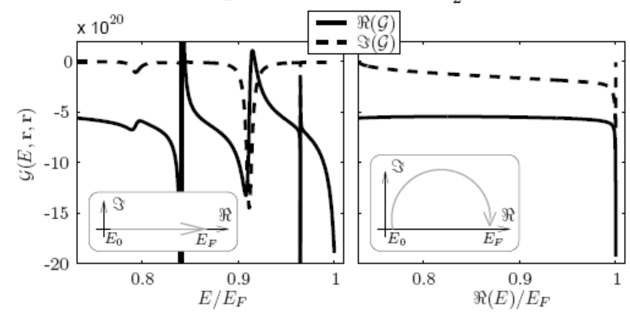

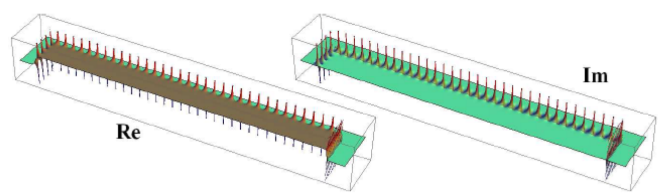

NEW:

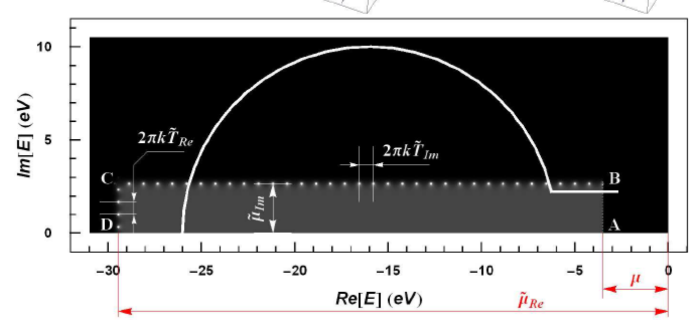

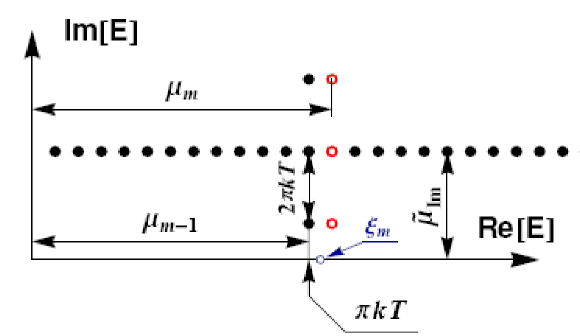

Gate Voltage Effect in All Carbon-Hydrogen GNRFET Composed of ~7000 Atoms

Zero Gate Voltage　　　　Gate Voltage -3 V

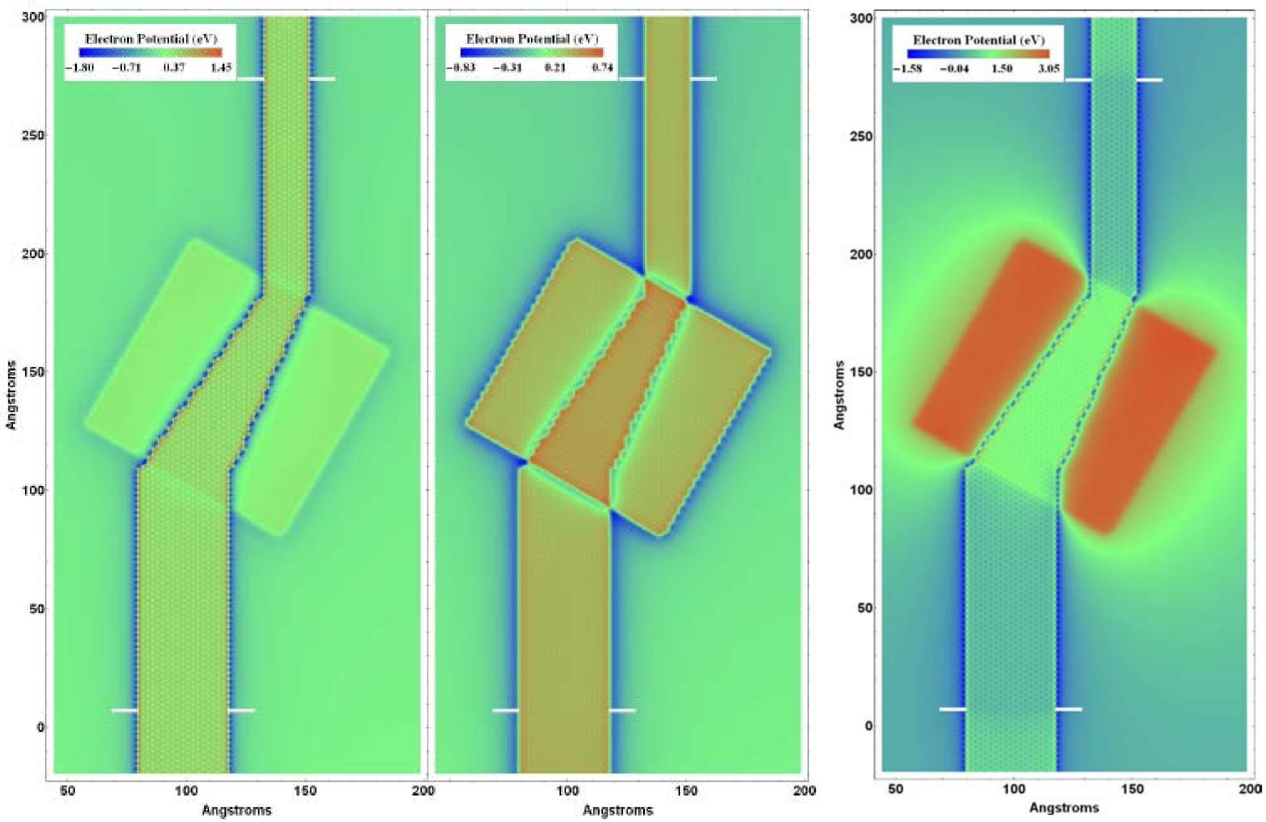

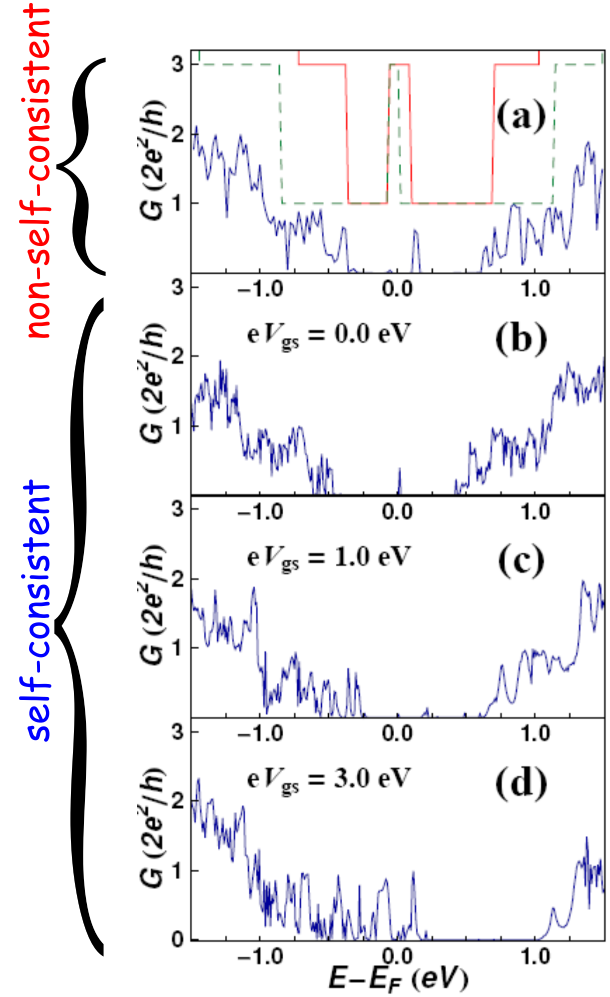

Nikolić group, PRB **81**, 155450 (2010)

NEGF-DFT For Multiterminal Devices

Saha et al., J. Chem. Phys. **131**, 164105 (2009)

$$D = -\frac{1}{\pi}\int_{-\infty}^{\infty} dE\, \mathrm{Im}\left[\mathrm{G}(E) f(E-\mu_m)\right] + \sum_{j\neq m}\int_{-\infty}^{\infty} dE\, \rho^j(E)\left[f(E-\mu_j) - f(E-\mu_m)\right]$$

$$\rho^i = \mathrm{G}(E)\Gamma_i(E)\mathrm{G}^\dagger$$

$$\tilde{D} = D^1 + \Delta^{12} + \Delta^{13}$$

$$D^1 = -\frac{1}{\pi}\int_{-\infty}^{\infty} dE\, \mathrm{Im}\left[G(E)\, f(E-\mu_1)\right]$$

$$\Delta^{12} = \int_{-\infty}^{\infty} dE\, \rho^2(E)\left[f(E-\mu_2) - f(E-\mu_1)\right]$$

$$\Delta^{13} = \int_{-\infty}^{\infty} dE\, \rho^3(E)\left[f(E-\mu_3) - f(E-\mu_1)\right]$$

$$\tilde{D} = D^2 + \Delta^{21} + \Delta^{23} \qquad \cdots \quad \cdots \quad \cdots$$

$$D^2 = -\frac{1}{\pi}\int_{-\infty}^{\infty} dE\, \mathrm{Im}\left[G(E)\, f(E-\mu_2)\right]$$

$$\Delta^{21} = \int_{-\infty}^{\infty} dE\, \rho^1(E)\left[f(E-\mu_1) - f(E-\mu_2)\right]$$

$$\Delta^{23} = \int_{-\infty}^{\infty} dE\, \rho^3(E)\left[f(E-\mu_3) - f(E-\mu_2)\right]$$

$$D = w^1\left(D^1 + \Delta^{12} + \Delta^{13}\right) + w^2\left(D^2 + \Delta^{21} + \Delta^{23}\right) + w^3\left(D^3 + \Delta^{31} + \Delta^{32}\right)$$

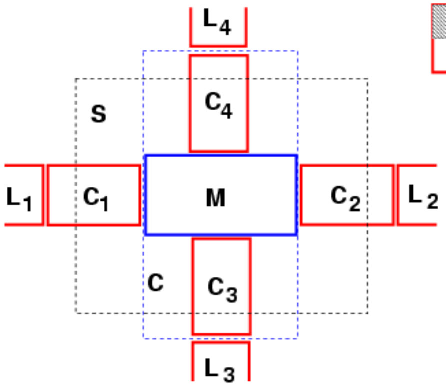

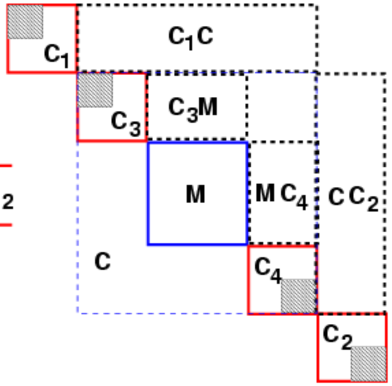

$$H = \begin{pmatrix} H_{\mathrm{C}_1} + \Sigma_{\mu_1} & 0 & V_{\mathrm{C}_1\mathrm{M}} & 0 & 0 \\ 0 & H_{\mathrm{C}_3} + \Sigma_{\mu_3} & V_{\mathrm{C}_3\mathrm{M}} & 0 & 0 \\ V_{\mathrm{MC}_1} & V_{\mathrm{MC}_3} & H_{\mathrm{M}} & V_{\mathrm{MC}_4} & V_{\mathrm{MC}_2} \\ 0 & 0 & V_{\mathrm{C}_4\mathrm{M}} & H_{\mathrm{C}_4} + \Sigma_{\mu_4} & 0 \\ 0 & 0 & V_{\mathrm{C}_2\mathrm{M}} & 0 & H_{\mathrm{C}_2} + \Sigma_{\mu_2} \end{pmatrix}$$

$$I_\alpha = \frac{2e}{h}\sum_{\beta\neq\alpha}\int dE\, T(E, V_\beta, V_\alpha)\left[f(E-\mu_\beta) - f(E-\mu_\alpha)\right]$$

Phonon Thermal Conductance via NEGF Coupled to Minimal Force Constant 4NNN Model

❑Phonon conductance:

$$\kappa_{\rm ph} = \frac{\hbar^2}{2\pi k_B T^2}\int_0^\infty d\omega\, \omega^2 \mathcal{T}_{\rm ph}(\omega)\frac{e^{\hbar\omega/k_BT}}{(e^{\hbar\omega/k_BT}-1)^2}$$

$$\mathcal{T}_{\rm ph}(\omega) = {\rm Tr}\left\{\mathbf{\Lambda}_L(\omega)\mathbf{G}(\omega)\mathbf{\Lambda}_R(\omega)\mathbf{G}^\dagger(\omega)\right\}$$
$$\mathbf{G}(\omega) = [\omega^2\mathbf{M}-\mathbf{K}-\mathbf{\Pi}_L(\omega)-\mathbf{\Pi}_R(\omega)]^{-1}$$

❑Why no phonon-phonon scattering? $W \ll \ell \approx 677\ {\rm nm}$ at 300 K [APL **98**, 141919 (2011)]

❑Empirical 4NNN force constant matrix:

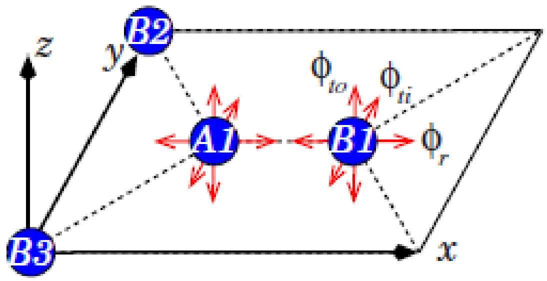

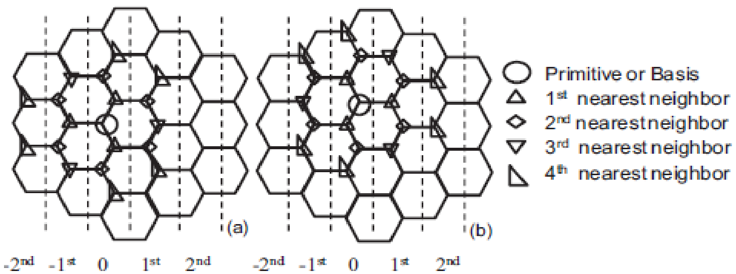

$$K_{A1,n} = \begin{pmatrix} \phi_{\rm r}^{(n)} & 0 & 0 \\ 0 & \phi_{\rm ti}^{(n)} & 0 \\ 0 & 0 & \phi_{\rm to}^{(n)} \end{pmatrix}$$

TABLE I. Force-constant parameters for graphene in units of 10^4 dyn/cm=10 N/m.

	Parameters by Saito *et al.* (Ref. 38)			Our parametrization		
Neighbor shell	$\phi_{\rm r}^{(n)}$	$\phi_{\rm ti}^{(n)}$	$\phi_{\rm to}^{(n)}$	$\phi_{\rm r}^{(n)}$	$\phi_{\rm ti}^{(n)}$	$\phi_{\rm to}^{(n)}$
First	36.50	24.50	9.82	41.8	15.2	10.2
Second	8.80	−3.23	−0.40	7.6	−4.35	−1.08
Third	3.00	−5.25	0.15	−0.15	3.39	1.0
Fourth	−1.92	2.29	−0.58	−0.69	−0.19	−0.55

$$\phi_t^{(1)} + 6\phi_t^{(2)} + 4\phi_t^{(3)} + 14\phi_t^{(4)} = 0$$

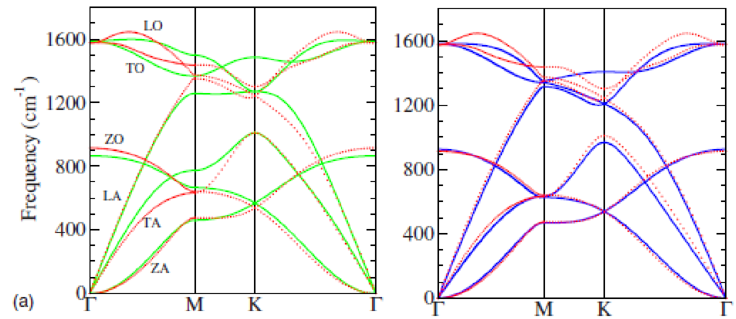

PRB **78**, 045410 (2008)

Phonon Thermal Conductance via NEGF Coupled to Brenner Empirical Potential or DFT

- Brenner empirical interatomic potential for hydrocarbon systems (GULP or GPAW):

PRB **81**, 205441 (2010)

$$V_{ij} = f^C_{ij}(f^R_{ij} - \bar{b}_{ij} f^A_{ij}), \quad \bar{b}_{ij} = \frac{1}{2}(b^{\sigma-\pi}_{ij} + b^{\sigma-\pi}_{ji}) + \Pi^{RC}_{ij} + b^{DH}_{ij},$$

$$f^R_{ij} = \left(1 + \frac{Q}{r_{ij}}\right) A e^{-\alpha r_{ij}}, \qquad b^{\sigma-\pi}_{ij} = \left(1 + \sum_{k \neq i,j} f^C_{ik} g_{ijk}\right)^{-1/2},$$

$$f^A_{ij} = \sum_{n}^{3} B_n e^{-\lambda_n r_{ij}}, \qquad g_{ijk} = \sum^{5} \beta_i \cos^i[\theta_{ijk}].$$

$$b^{DH}_{ij} = \frac{T_0}{2} \sum_{k,l \neq i,j} f^C_{ik} f^C_{jl} (1 - \cos^2[\Theta_{ijkl}])$$

$$K_{I\alpha,J\beta} = \partial V / (\partial R_{I\alpha} \partial R_{J\beta})$$

The Brenner EIPs are short range, so they cannot accurately fit the graphene dispersion over the entire BZ. However, the thermal transport depends more sensitively on the accuracy of acoustic phonon frequencies near the zone center where the longitudinal- and transverse-acoustic (LA and TA) velocities and the quadratic curvature of the out-of-plane acoustic (ZA) branch are determined. Conversely, only weak thermal excitation of the optical phonons and acoustic phonons near the BZ boundary occurs around room temperature because of the large Debye temperature (~ 2000 K) of graphene.

- First-principles brute force method to obtain the force constant matrix (GPAW):

we displace each atom I by $Q_{I\alpha}$ in the direction α={x,y,z} to get the forces $F_{I\alpha,J\beta}$ on atom J$\neq$ I in direction β

$$K_{I\alpha,J\beta} = [F_{J\beta}(Q_{I\alpha}) - F_{J\beta}(-Q_{I\alpha})]/2Q_{I\alpha}$$

$$K_{I\alpha,I\beta} = -\Sigma_{J \neq I} K_{I\alpha,J\beta}$$

for intra-atomic elements impose momentum conservation

Which Method Should You Use: Minimal 4NNNFC vs. Brenner EIP vs. DFT

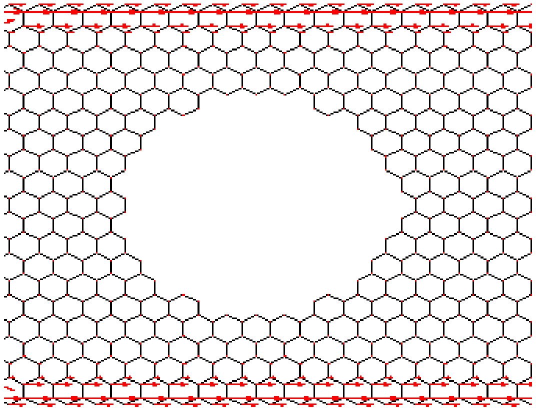

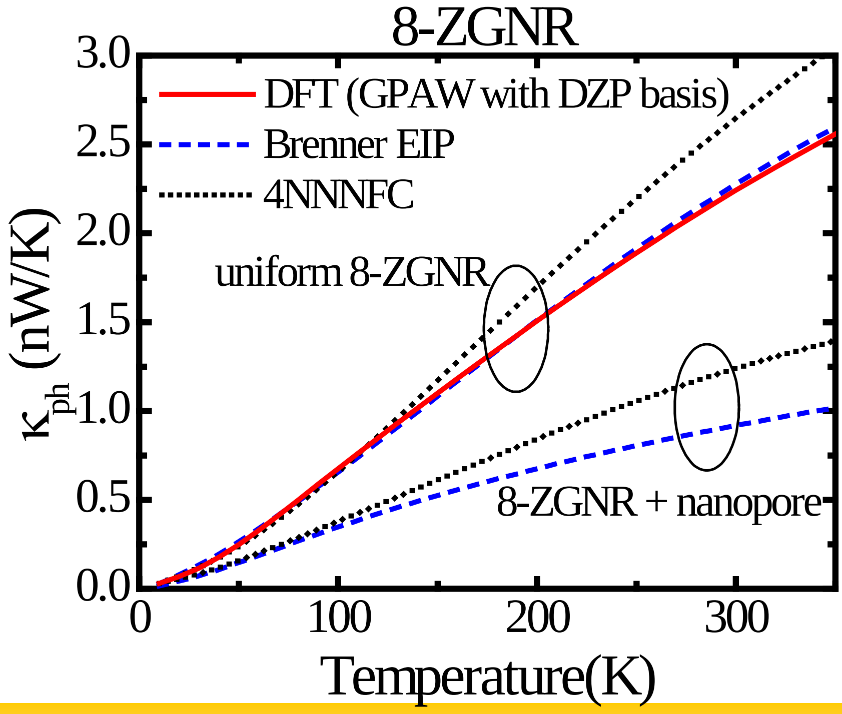

ZGNR|18-annulene|ZGNR

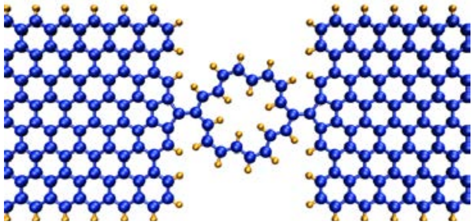

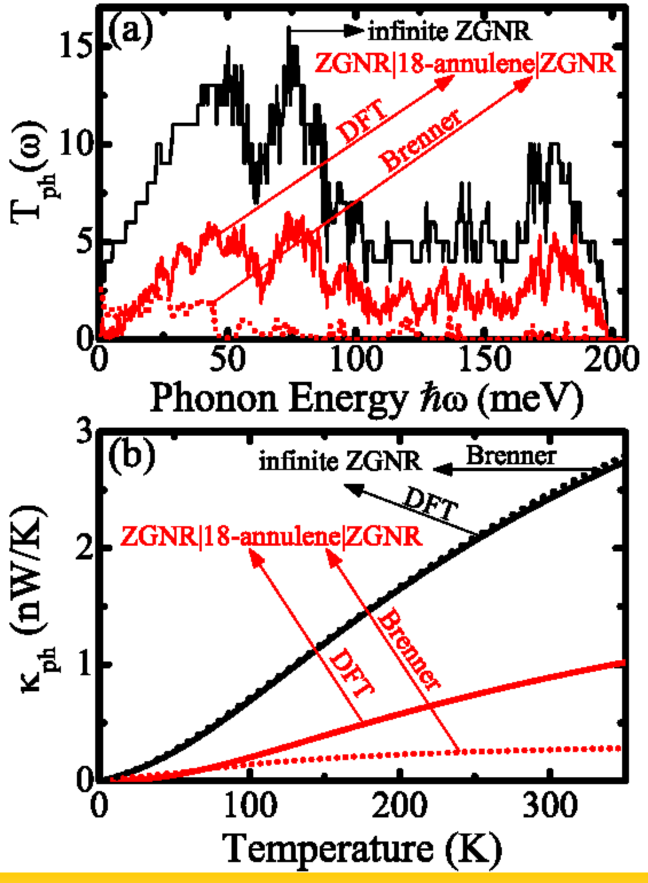

Electron and Phonon Transport in ZGNRs and CGNRs with Nanopores

Nikolic group, arXiv:1201.1665

$L \simeq 1.2\ \mu m$

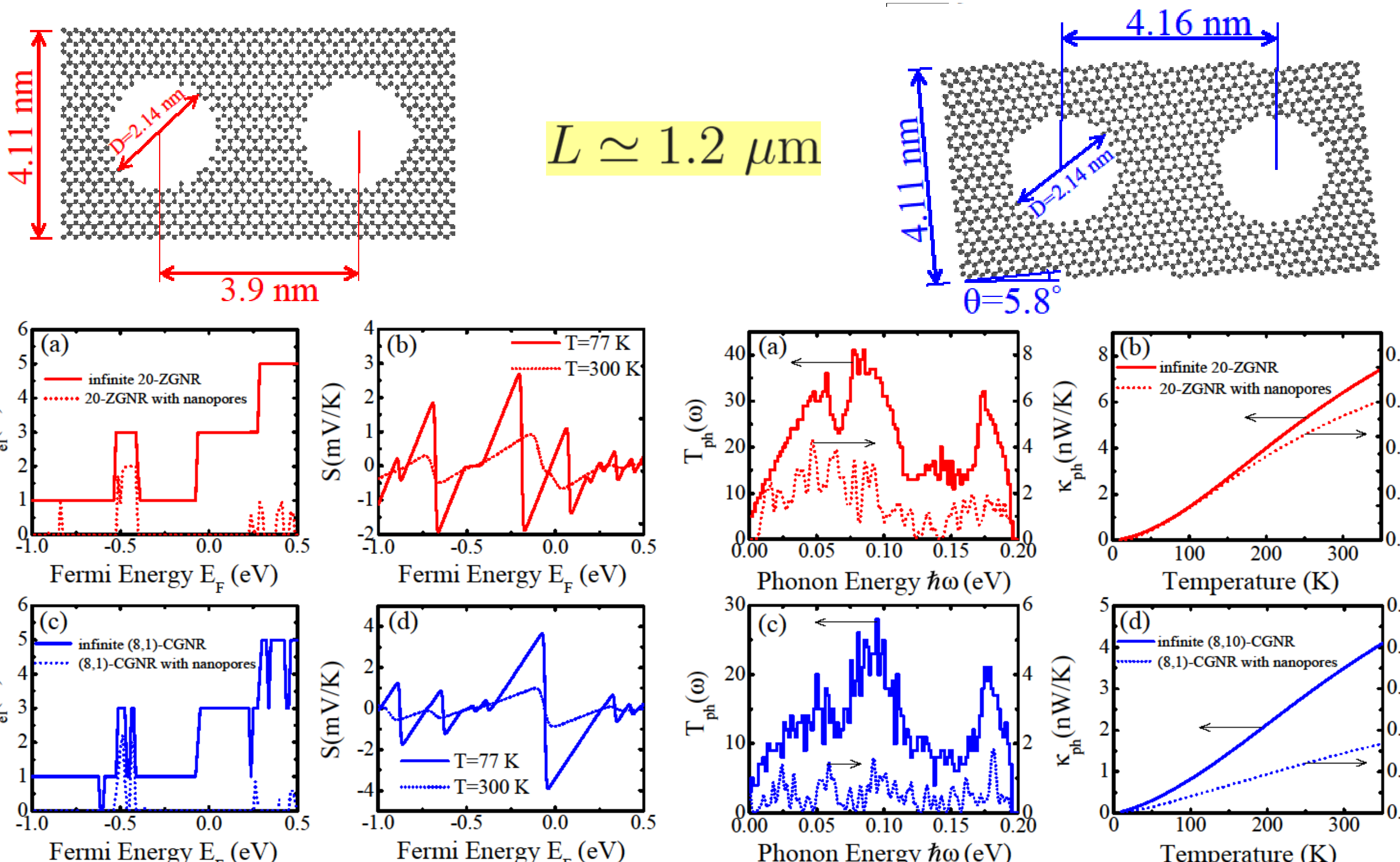

Graphene-Based Topological Insulators with Nanopores as Thermoelectric

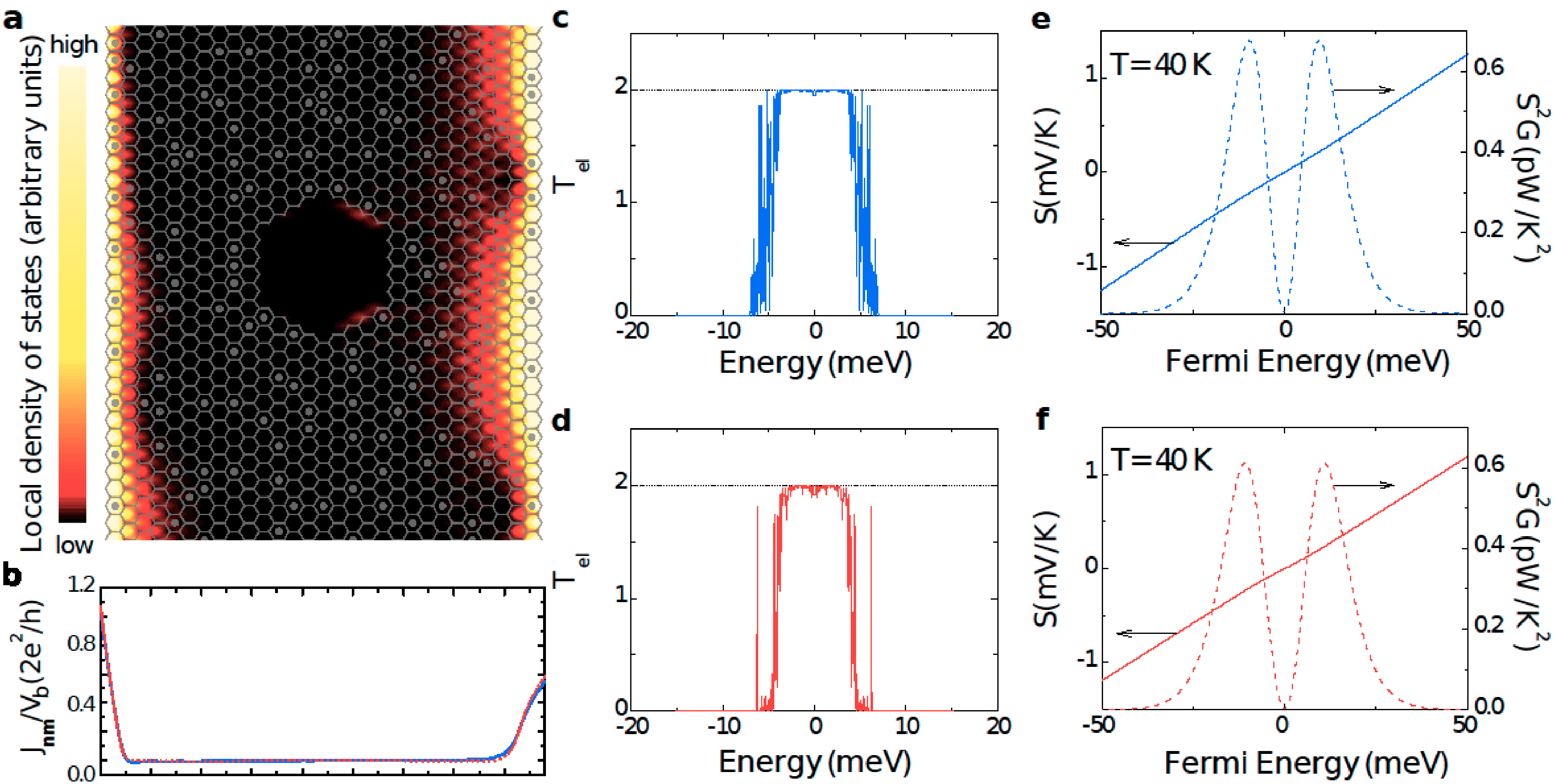

Graphene-Based Topological Insulators with Nanopores as Thermoelectric

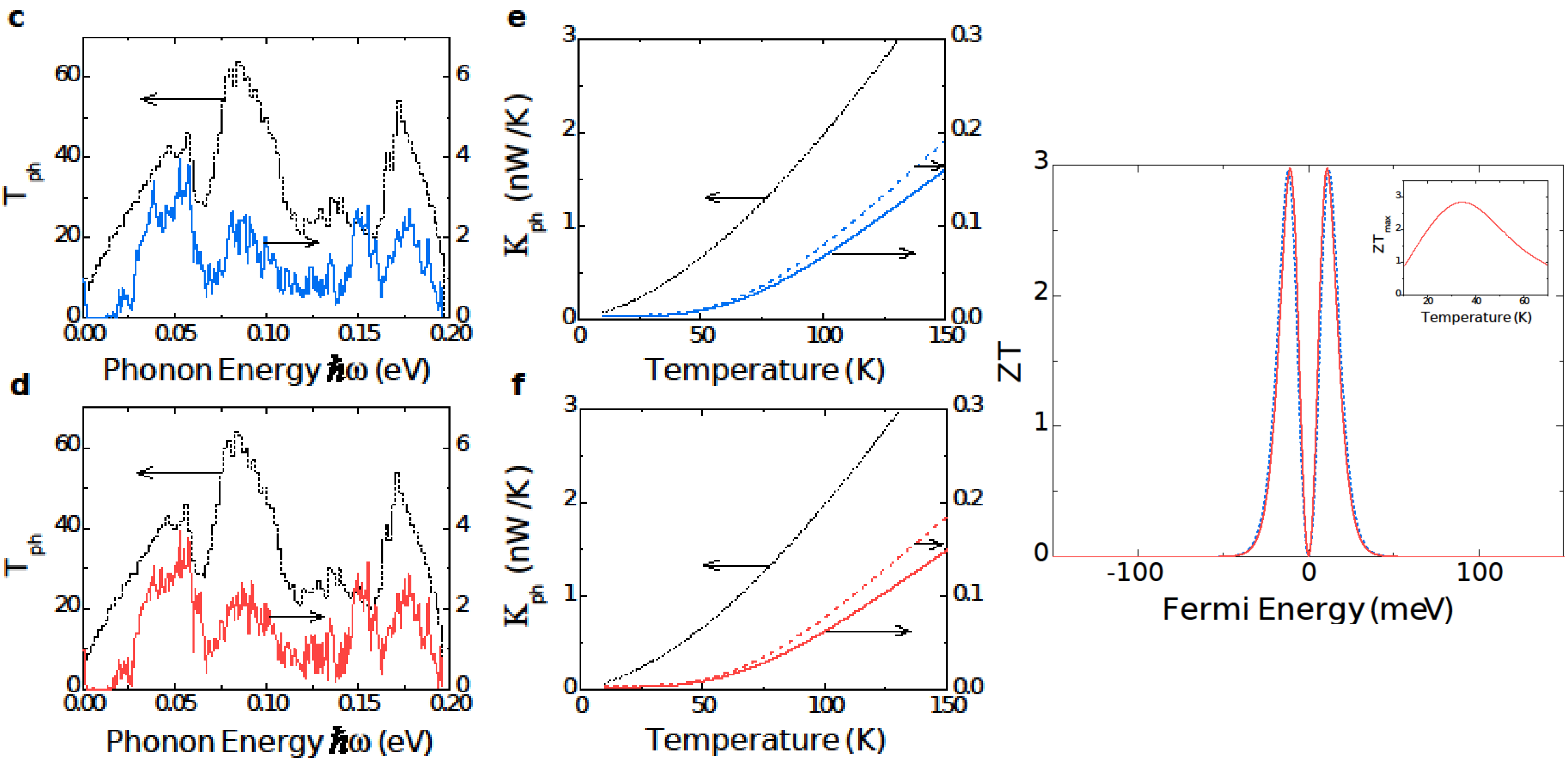

Thermoelectricity in Single-Molecule Nanojunctions

Majumdar Lab, Science **315**, 2568 (2007)

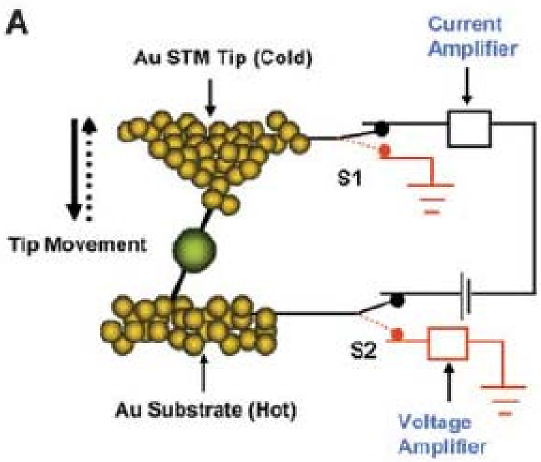

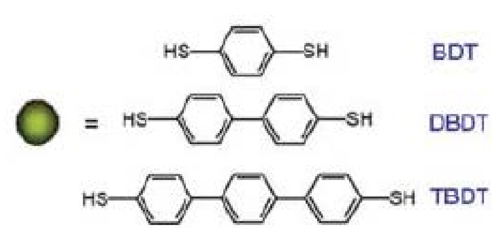

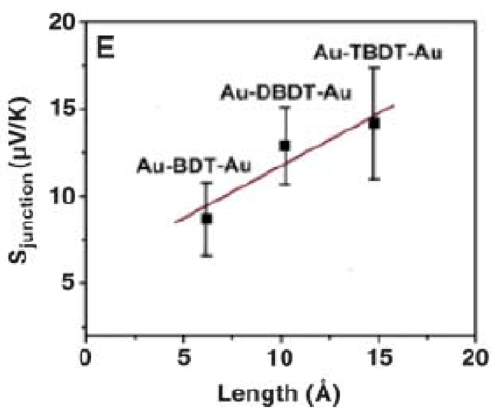

Cuniberti group, PRB **81**, 235406 (2010)

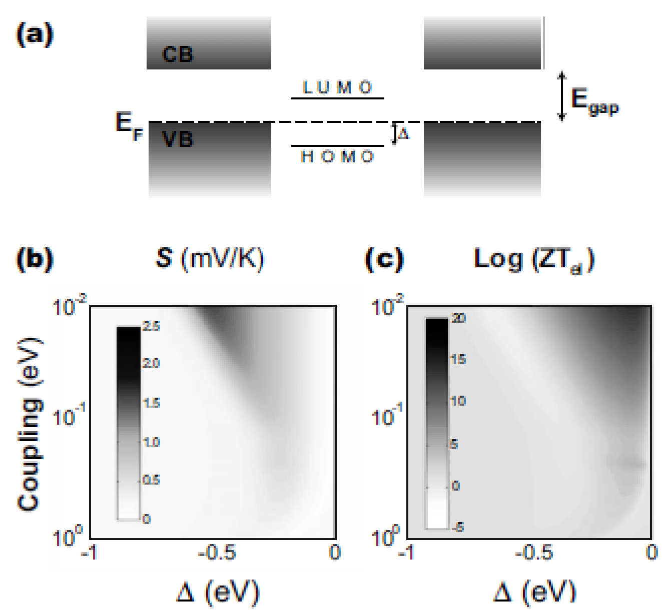

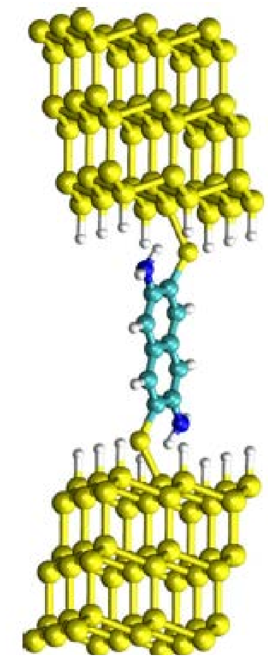

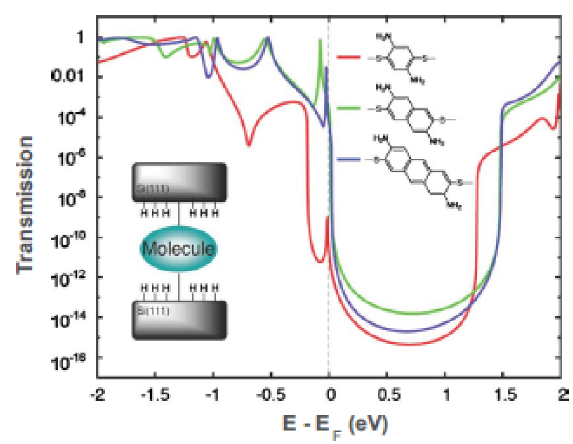

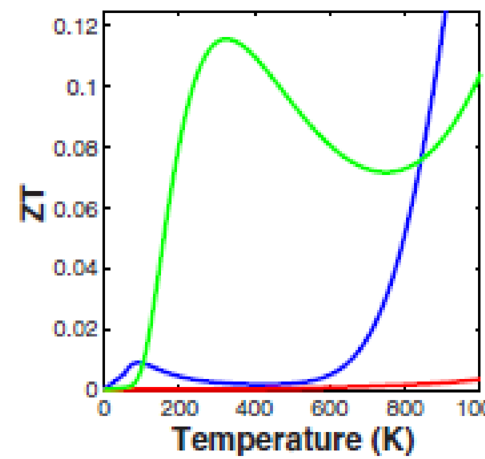

Toward Metal-Free Molecular Electronics

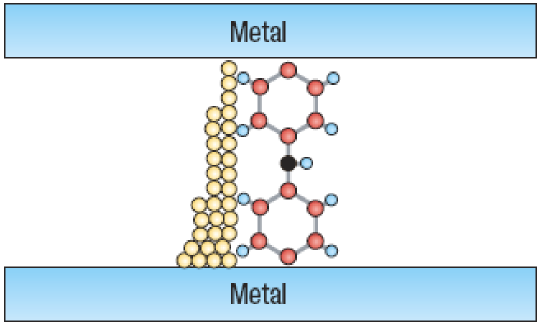

❑Control of the contact structure between an organic molecule and a metal electrode (usually gold) is difficult because bonding to metal atoms, although potentially strong, **is not strongly directional**, leading to **poor reproducibility** of most metal-molecule-metal junctions.

Nature. Mater. **5**, 63 (2006)

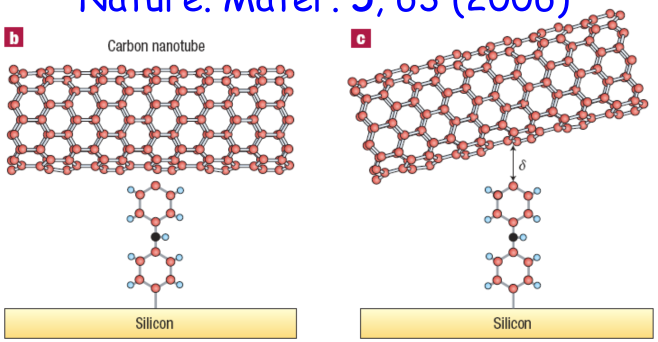

Science **311**, 356 - 359 (2006)

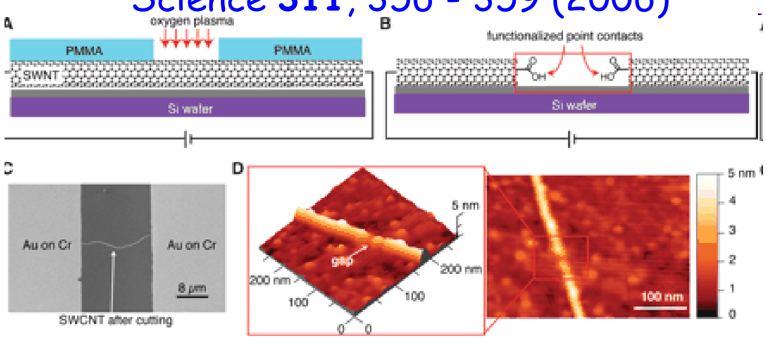

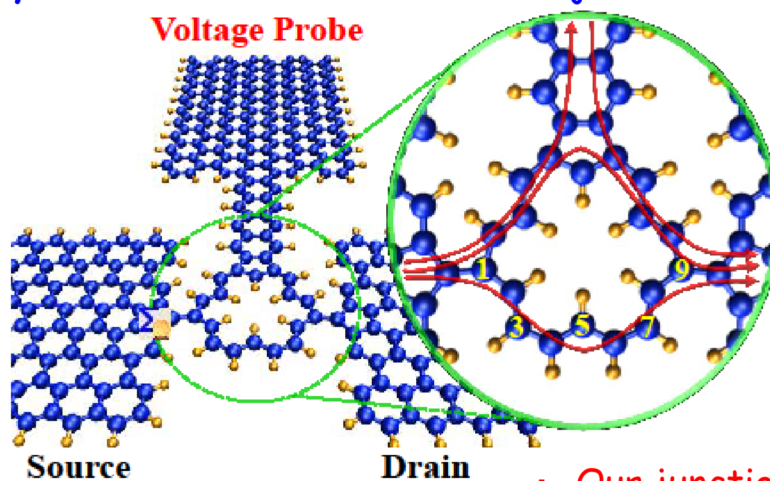

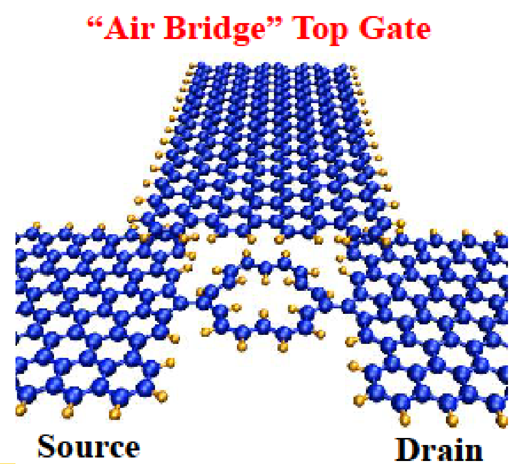

Our junctions with strong molecule-electrode coupling evade problems due to the lack of **derivative discontinuity** in continuous local and semi-local DFT approximations (LDA and GGA) as a **major source of error** in calculating the *I*-*V* characteristics

Nikolić group, PRL **100**, 236803 (2010)

ZGNR|molecule|ZGNR Thermoelectric Devices Based on Evanescent Mode Transport

ZGNR|18-annulene|ZGNR

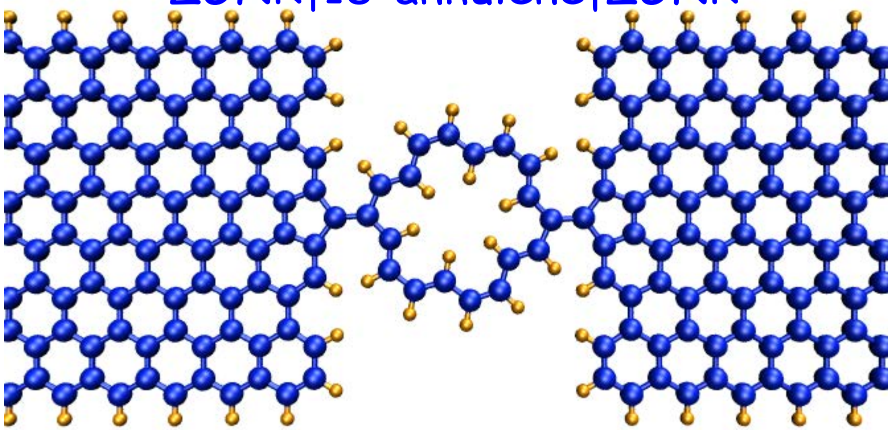

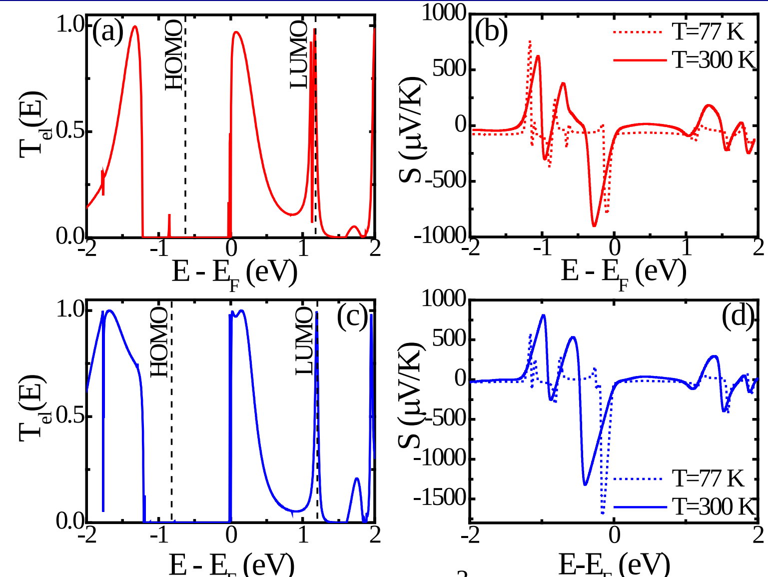

Nikolić group, PRB **84**, 041412(R) (2011)
+ J. Comp. Electronics **11**, 78 (2012)

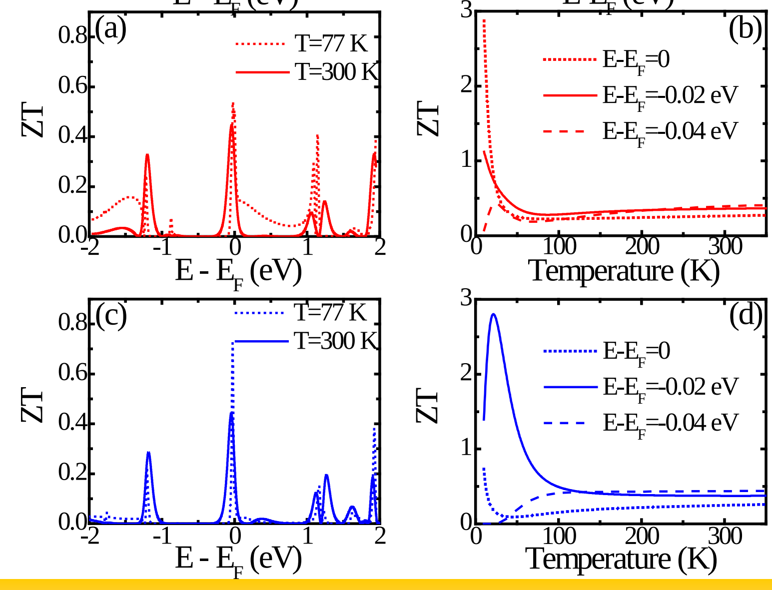

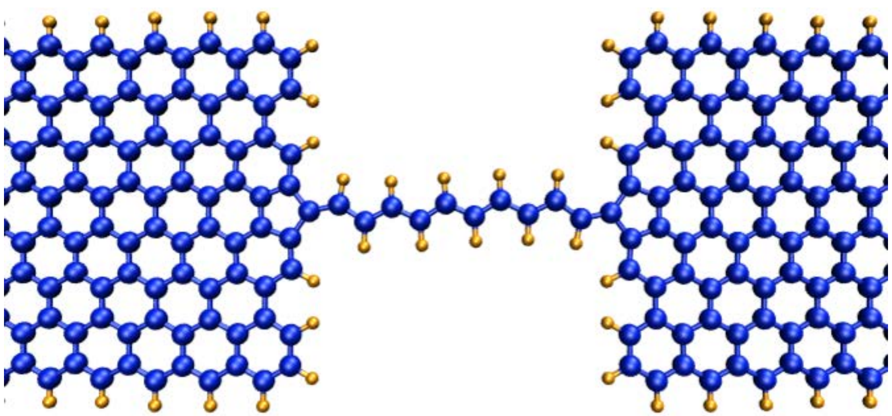

ZGNR|C10|ZGNR

Three-Terminal Single-Molecule Nanojunction Thermoelectrics

Nikolić group, PRB **84**, 041412(R) (2011)

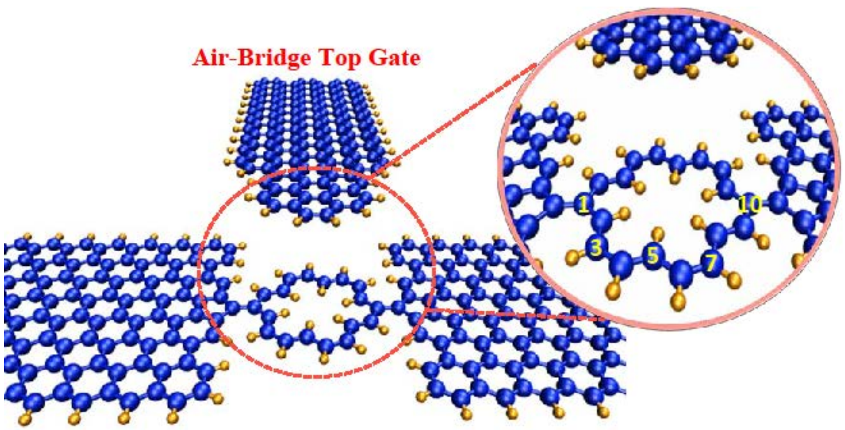

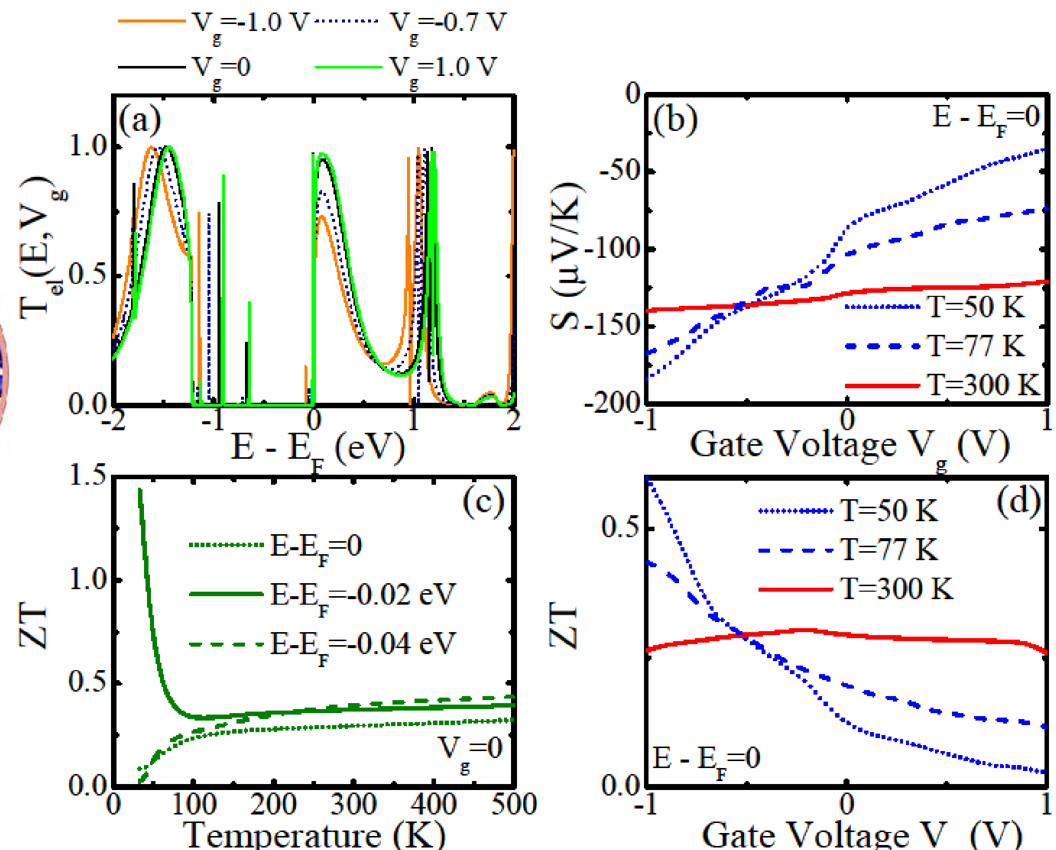

Fabrication of Single-Molecule Nanojunctions with Graphene Electrodes

van der Zant Lab, Nano Lett. **11**, 4607 (2011)

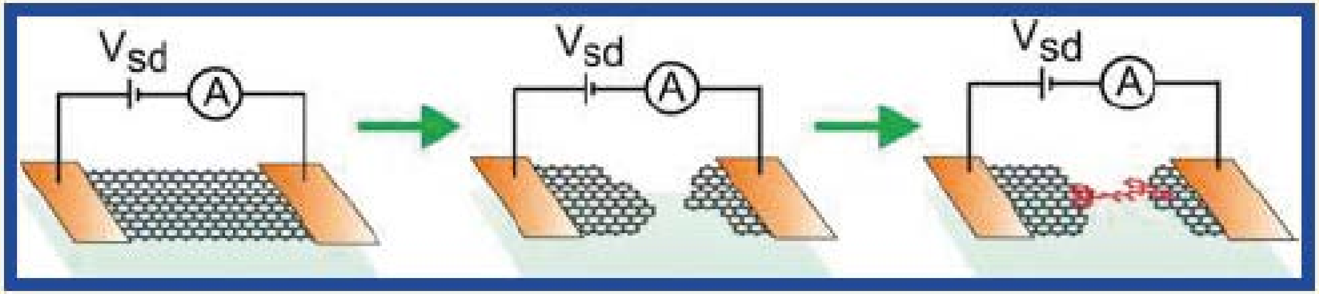

depositing molecules inside a few-layer graphene nanogap (of the size 1-2 nm) formed by feedback controlled electroburning

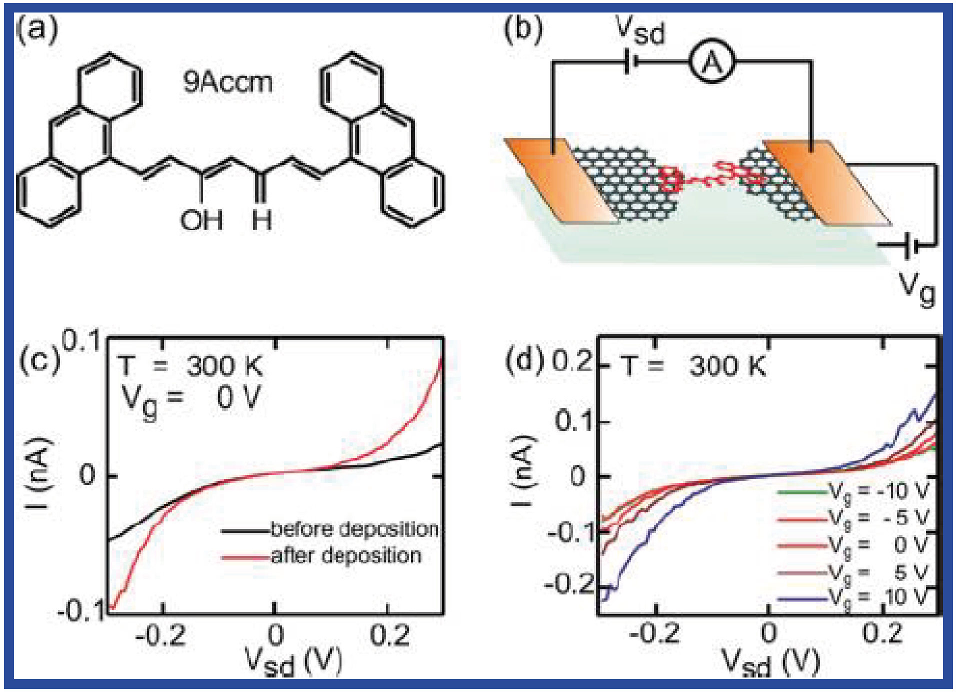

Gatable I-V characteristics at room temperature

Coupled Electron-Phonon Transport via NEGF

$$\hat{H} = \hat{H}_{\text{e}}^{0} + \hat{H}_{\text{ph}}^{0} + \hat{H}_{\text{e-ph}} = \sum_{i,j} H_{ij}^{0}\hat{c}_i^{\dagger}\hat{c}_j + \sum_{i,j} \hbar\omega_{\lambda}\hat{a}_{\lambda}^{\dagger}\hat{a}_{\lambda} + \sum_{\lambda,i,j} M_{ij}^{\lambda}\hat{c}_i^{\dagger}\hat{c}_j(\hat{a}_{\lambda}^{\dagger} + \hat{a}_{\lambda})$$

empirical models or DFT (GPAW) computed

(a)

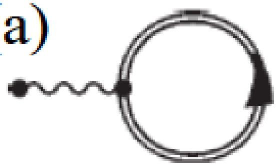

$$\Sigma^{H} = i\sum_{\lambda}\frac{2}{\omega_{\lambda}}\int\frac{dE'}{2\pi}\mathbf{M}^{\lambda}\mathrm{Tr}\left[\mathbf{G}_0^{<}(E')\mathbf{M}^{\lambda}\right]$$

$$\Sigma^{H,<} = 0$$

(b)

$$\Sigma^{F}(E) = i\sum_{\lambda}\int\frac{dE'}{2\pi}\mathbf{M}^{\lambda}\begin{bmatrix}\mathbf{D}_0(E-E')\mathbf{G}_0^{<}(E') + \mathbf{D}_0(E-E')\mathbf{G}_0(E') \\ +\mathbf{D}_0^{<}(E-E')\mathbf{G}_0(E')\end{bmatrix}\mathbf{M}^{\lambda}$$

$$\Sigma^{F,<}(E) = i\sum_{\lambda}\int\frac{dE'}{2\pi}\mathbf{M}^{\lambda}\mathbf{D}_0(E-E')\mathbf{G}_0^{<}(E')\mathbf{M}^{\lambda}$$

electron self-energies in SCBA

(c)

$$\Pi(\omega) = -i\sum_{\lambda}\int\frac{dE'}{2\pi}\mathbf{M}^{\lambda}\begin{bmatrix}\mathbf{G}_0(E')\mathbf{G}_0^{<}(E'-\omega) + \\ \mathbf{G}_0^{<}(E)\mathbf{G}_0^{\dagger}(E'-\omega)\end{bmatrix}\mathbf{M}^{\lambda}$$

$$\Pi^{<}(\omega) = -i\sum_{\lambda}\int\frac{dE'}{2\pi}\mathbf{M}^{\lambda}\mathbf{G}_0^{<}(E)\mathbf{G}_0^{>}(E'-\omega)\mathbf{M}^{\lambda}$$

phonon self-energies in SCBA

second-order diagrams

(d)

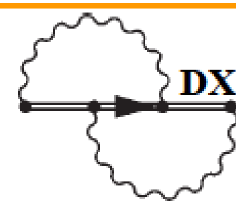

(e)

- Phonon drag: $S = S_{\text{el}} + S_{\text{ph}}$ arises due to interchange of momentum between acoustic phonons and electrons
- Electron drag: phonons are dragged by electrons from low into high T region

- Three- and four-phonon many-body interactions

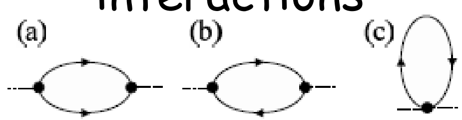

PRB 74, 125402 (2006)

New Routes for ZT Optimization Brought by Low-Dimensional and Nanoscale Devices

Transmission peaks or nodes

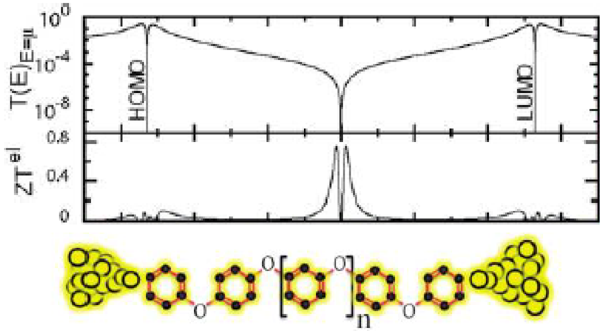

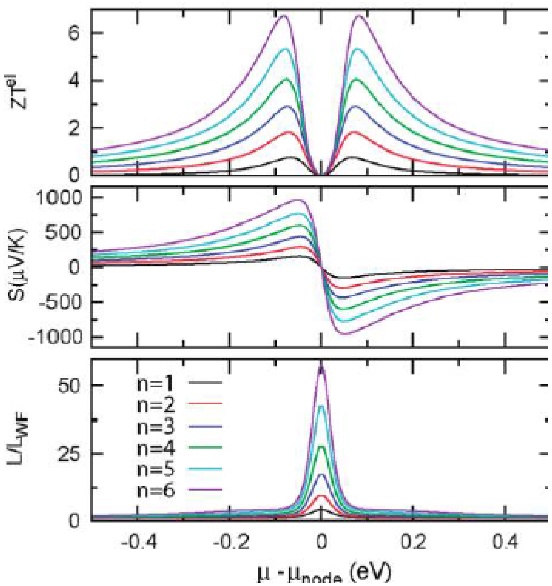

$$L = \kappa_{\rm el}/GT$$
$$L_{\rm WF} = \pi^2/3(k_B/e)^2$$

ACS Nano **4**, 5314 (2010)

Coulomb interaction

PRB **78**, 161406(R) (2008)

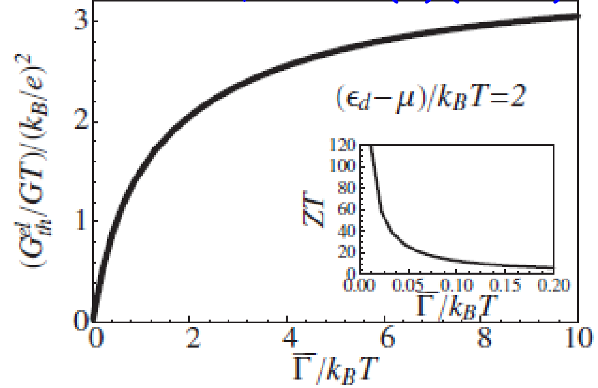

Nonlinear regime

PRB **82**, 045412 (2010)

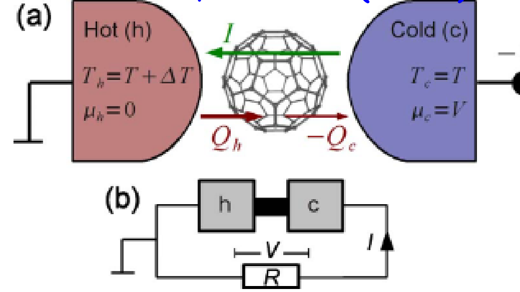

$$\eta = IV/Q_h$$

Electron-phonon coupling

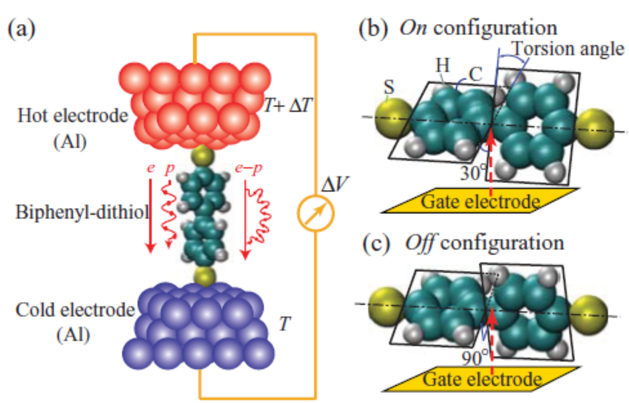

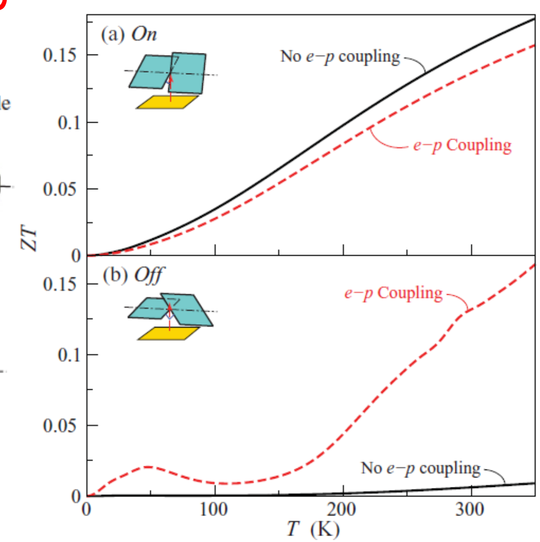

PR B **83**, 195415 (2011)

Conclusions in Pictures

Edge currents and nanopores in GNR thermoelectrics:

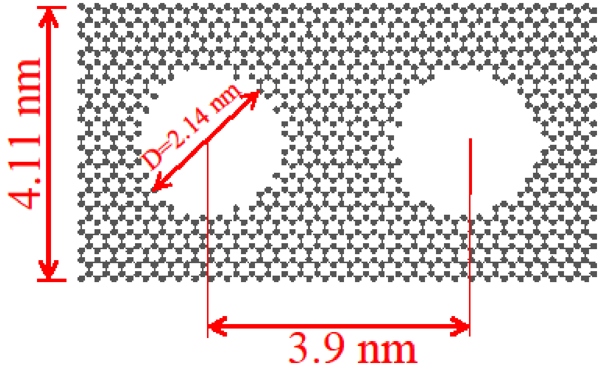

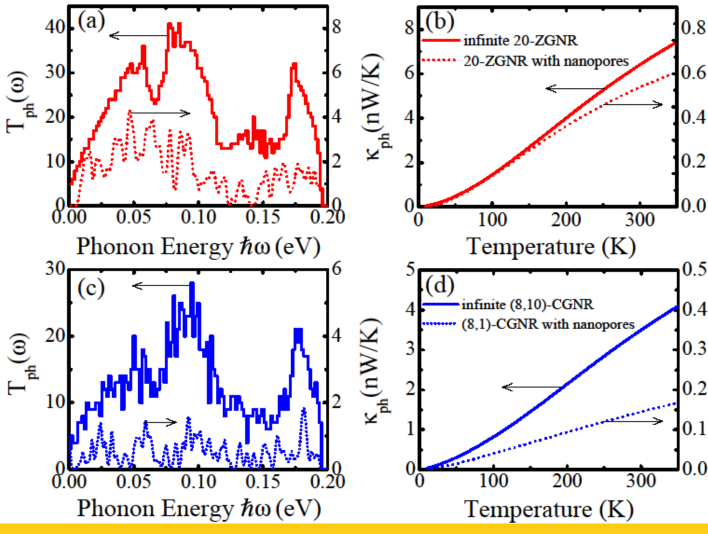

Evanescent mode transport in single-molecule nanojunctions to optimize power factor:

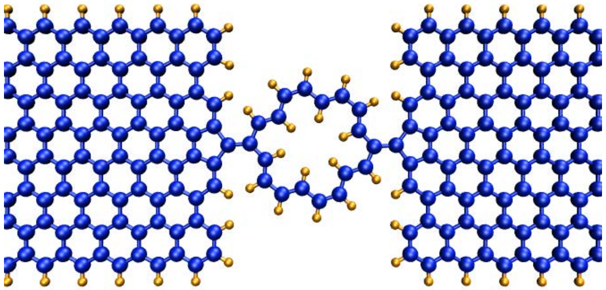

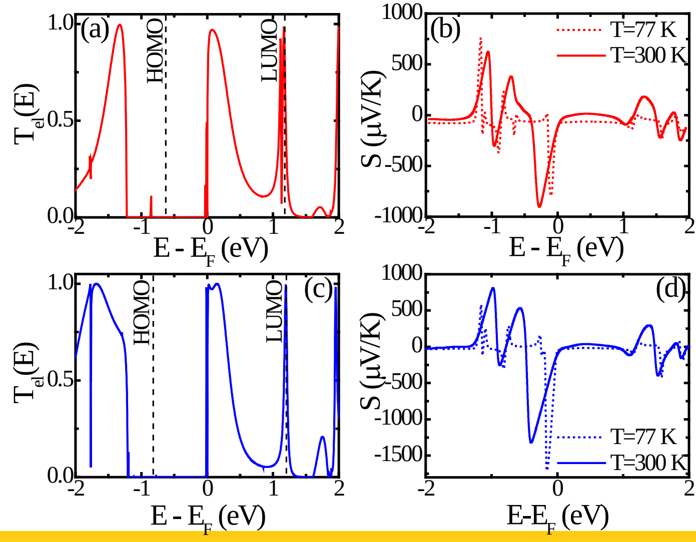

Complete separation of electronic and phononic transport in 2D TIs: